Could residential air-source heat pumps exacerbate outdoor summer overheating and winter overcooling in UK 2050s climate scenarios?

Sustainable Cities and Society 115 (2024) 105811

Contents lists available at ScienceDirect

Sustainable Cities and Society

journal homepage: www.elsevier.com/locate/scs

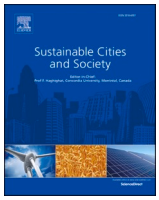

Could residential air-source heat pumps exacerbate outdoor summer overheating and winter overcooling in UK 2050s climate scenarios?

Xiaoxiong Xie [a,b], Zhiwen Luo [b,*], Sue Grimmond [c], Yiqing Liu [d], Carlos E. Ugalde-Loo [e], Matthew T. Bailey [f], Xinfang Wang [g]

[a] School of Art, Design and Architecture, University of Plymouth, United Kingdom
[b] Welsh School of Architecture, Cardiff University, United Kingdom
[c] Department of Meteorology, University of Reading, United Kingdom
[d] School of the Built Environment, University of Reading, United Kingdom
[e] School of Engineering, Cardiff University, United Kingdom
[f] School of Geography, Earth and Environmental Sciences, University of Plymouth, United Kingdom
[g] School of Chemical Engineering, University of Birmingham, United Kingdom

ARTICLE INFO

Keywords:
Urban heat island
Net zero emissions
Climate resilience
EnergyPlus
SUEWS

ABSTRACT

The UK government promotes heat pumps to replace gas boilers in the residential sector as a vital part of its strategy to achieve Net Zero by 2050. As climate change intensifies, heat pumps, traditionally used for heating, will also play a role in cooling to address indoor heat risks that threaten public health and increase energy demands. However, air-source heat pumps (ASHPs) might unintentionally exacerbate summer overheating and winter overcooling in residential neighbourhoods. This study uses a multi-scale modelling approach, combining SUEWS and EnergyPlus, to assess the impact of ASHPs on outdoor temperature in two idealised UK low-rise residential neighbourhoods under 2050s climate scenarios. Results show that in summer, ASHPs increase median anthropogenic heat emission by up to 19.3 W m^{-2} and raise local median 2 m air temperature by up to 0.12 °C in an idealised London neighbourhood. In winter, replacing gas boilers with ASHPs for heating reduces anthropogenic heat emissions by up to 11.1 W m^{-2} and lowers local air temperatures by up to 0.16 °C in London. The research shows that conventional waste heat calculations from air-conditioning can overestimate anthropogenic heat emissions by up to 86 %, and cooling entire building rather than just occupied rooms can increase energy consumption by 68 %. Although temperature changes will vary across UK cities, the response of air temperature to anthropogenic heat change is generally consistent. The study enhances understanding of role of ASHPs in the UK's net zero target for 2050, highlighting the importance of balancing outdoor and indoor thermal comfort when considering the wide use of ASHPs.

1. Introduction

The energy sector is a major contributor to greenhouse gas emissions and climate change. It is responsible for more than two-thirds of global emissions (World Resources Institute, 2022). The building sector, plays a notable role, consuming 30 % of the world's final energy and producing 27 % of the energy sector's carbon emissions (IEA, 2022a). However, potential exists to reduce this by adopting more efficient and cleaner heating solutions. Heat pumps are an available technology that have received significant support globally. In simple terms, heat pumps use electrical energy to transfer heat from a colder space (outdoors) to a warmer space (indoors) when used for heating purpose (Chua et al., 2010).

The global heat pumps market is expanding, with marked increases in North America, Europe, and Asia (IEA, 2022b). By 2021, 190 million units were in operation worldwide (IEA, 2022b). The International Energy Agency (IEA) has an ambitious goal of fulfilling 50 % of the global heating requirements with heat pumps by 2045 (IEA, 2021). Similarly, the UK aims to achieve net-zero carbon emissions by 2050, requiring reforms across all energy-consuming sectors (BEIS, 2021). Residential heating accounts for approximately 13 % of the UK's total greenhouse gas emissions (UKERC, 2020), primarily as gas boilers are used by 85 % of households (UKERC, 2016). Thus, decarbonising this sector is critical, especially given the increase in home working post-pandemic. The UK Climate Change Committee (2020) estimates that achieving net zero will require domestic heat pumps to be installed in 50 % to 80 % of homes by

* Corresponding author at: Bute Building, Room 1.23, King Edward VII Avenue, Cardiff, CF10 3NB, United Kingdom.
E-mail address: LuoZ18@Cardiff.ac.uk (Z. Luo).

https://doi.org/10.1016/j.scs.2024.105811
Received 31 May 2024; Received in revised form 20 August 2024; Accepted 8 September 2024
Available online 12 September 2024

Nomenclature

T_2	Outdoor 2 m air temperature (°C)
T_b	Base temperature for cooling/heating degree days calculation (°C)
Q^*	Net all-wave radiation (W m^{-2})
Q_E	Latent heat flux (W m^{-2})
Q_{EC}	Energy consumption of heating/cooling system (W m^{-2})
Q_F	Anthropogenic heat flux (W m^{-2})
$Q_{F,B}$	Building anthropogenic heat flux (W m^{-2})
Q_H	Sensible heat flux (W m^{-2})
$Q_{internal}$	Building internal heat gain (W m^{-2})
Q_S	Storage heat flux (W m^{-2})
Q_{waste}	Waste heat emission (W m^{-2})
ρ_{pop}	Population per hectare (cap ha^{-1})

2050, raising from <1 % currently (MHCLG, 2021). To support this, the UK government is promoting the adoption of residential heat pumps through subsidies such as the Boiler Upgrade Scheme (Department for Energy Security & Net Zero, 2023), positioning heat pumps to be the dominant technology in the UK's residential heating sector. Similarly, over 30 countries, which account for >70 % of global heating demand for buildings, have implemented incentive policies to subsidise heat pump installations (IEA, 2024).

With ongoing global warming, UK's climate is likely to change from being heating-focused to one needing both heating and cooling (Bastin et al., 2019). Projections for the 2050s suggest a 200 % increase in cooling demand compared to the 2020s (Chow et al., 2010). Hence, heat pump use is expected to expand from heating only to also include cooling. This shift requires an assessment of the cooling capabilities of heat pumps in the UK (BIES, 2021). As air source heat pumps (ASHP) cooling removes heat from indoors and release it outside, this could intensify urban heat island effects, particularly in densely populated areas. Conventional air-conditioning systems are known to have this issue (Table 1). While ASHPs have the potential to enable decarbonisation, the impact of urban overheating during summer cooling and overcooling in winter periods requires further investigation.

The role of air conditioners in raising 2 m outdoor air temperatures has been assessed in several cities via anthropogenic heat emissions increase with (cf. without) air-conditioning (Table 1). For instance, increases of up to 1.5 °C in Phoenix (Salamanca et al., 2014), 1.7 °C in New York (Gutiérrez et al., 2015), and 2 °C in Hong Kong (Wang et al., 2018) have been reported, with the latter linked to a 300 W m^{-2} increase in anthropogenic heat emissions. The magnitude of these heat emissions is influenced by factors such as the air conditioning systems efficiency and cooling demand. These increases, in turn, are affected by buildings characteristics (e.g. density, volume) and occupancy patterns (Salamanca et al., 2014), and atmospheric heat conductance/resistance feedbacks (Wang et al., 2023).

In addition to their summer cooling effects, ASHPs can also affect outdoor air temperatures in winter. By extracting heat from the outdoor air for indoor heating, ASHPs may reduce outdoor temperatures compared to the baseline scenario of gas boilers. This reduction in anthropogenic heat emissions during winter can potentially increase the heating load, offering a contrasting impact from their summer cooling effect. However, unlike the impact from summer cooling, this winter impact remains largely unstudied.

Around 18 % of households in the UK experience fuel poverty and cannot adequately heat their homes (Roberts et al., 2015). Currently active cooling is rare in UK homes (2 % air conditioner use rate) due to the mild climate (MHCLG, 2021). However, it is crucial to investigate the potential impact of government-promoted large-scale use of heat pumps for residential cooling and heating in future climate conditions. Since residential areas cover the largest portions of cities, the changes in urban air temperatures from air source heat pump may raise the risk of urban overheating and/or overcooling, elevate energy use and costs for households using active cooling and heating, and increase indoor overheating and/or overcooling risks for disadvantaged households. This situation could be worse for those unable to afford ASHPs or facing fuel poverty, thereby exacerbating social inequality and injustice (Lee et al., 2024).

Previous studies investigating the impact of air conditioning on local climate have employed the BEP/BEM (building effect parameterization/building energy modelling) framework within a meso-scale weather model (Kikegawa et al., 2003; Salamanca et al., 2010). Due to the high computational demands, simplifying assumptions are made, such as using uniform 'shoebox' structures that involve simple cubic geometries with only one single zone (Battini et al., 2023). The BEP/BEM framework compares well to the more detailed EnergyPlus building energy model (U.S. Department of Energy, 2020a) for the same 'shoebox' case (Pokhrel et al., 2019; Xu et al., 2018). However, it lacks detailed descriptions of building data, particularly regarding human behaviour inside the building.

EnergyPlus allows dynamic modelling of heat transfer and energy consumption in buildings, accounting for detailed building geometry (e.g. room and space configurations), occupant behaviour and system operation. Varied patterns of occupancy and air conditioning operations

Table 1
Studies documenting an increase in 2 m air temperature (ΔT_2) associated with heat emissions from air conditioners (ΔQ_F) compared to when no air conditioners are used, from which the ΔT_2 to $\Delta Q_{F,B}$ ratio at the time of the day when the maximum (peak) Q_F occurs (i.e. $\Delta T_2/\Delta Q_{F,B,peak}$) is estimated. If time of $\Delta Q_{F,\ peak}$ and ΔT_2 is not given, ratio is estimated from the largest daytime ΔQ_F and ΔT_2 values given. [a] Extra heat adding into the building making indoor temperature exceed the setpoint.

City	Study period	Model	Heat emission method	Spatial resolution (m)	$\Delta Q_{F,\ peak}$ (W m^{-2})	ΔT_2 at $\Delta Q_{F,\ peak}$ (°C)	$\Delta T_2/\Delta Q_{F,\ peak}$ (°C/W m^{-2})	Reference
Paris, France	8 – 13 Aug/ 2003	TEB	Waste heat [a]	250	900	1	0.0011	De Munck et al. (2013)
Phoenix, US	10 – 19 Jul/ 2009	WRF+BEP/BEM	Waste heat	1000	60	0.5	0.0083	Salamanca et al. (2014)
New York, US	3 – 8 Jul/2010	WRF+BEP/BEM	Waste heat	1000	160	1.7	0.0106	Gutiérrez et al. (2015)
Osaka, Japan	Jul – Sep/ 2013	1-D mixing-layer model	Observed energy consumption	By substation,mean 2.2 km^2	172	0.72	0.0042	Ohashi et al. (2016)
Hong Kong, China	23 – 28 Jun/ 2016	WRF+BEP/BEM	Waste heat	500	300	2	0.0067	Wang et al. (2018)
Osaka, Japan	Jul – Aug/ 2013	WRF+CM+BEM	Waste heat	1000	25	0.1	0.0040	Kikegawa et al. (2022)
Los Angeles	Jul/2018	WRF-UCM+EnergyPlus	Total building heat emission	450	100	0.02	0.0002	Xu et al. (2024)

at different times and in different spaces can be accounted for (Cuerda et al., 2019). It has been widely used to model the building heat emissions to outdoors (Chen et al., 2022; Ferrando et al., 2021; Hong et al., 2020; Liu et al., 2022). Conventionally and typically, EnergyPlus is used to simulate isolated buildings. However, by integrating it with urban climate models such as the Surface Urban Energy and Water Balance Scheme (SUEWS) (Tang et al., 2021; Xie et al., 2023b), the interaction between urban climate and building energy can be assessed.

Like BEP/BEM, SUEWS (Järvi et al., 2011; Ward et al., 2016) is a neighbourhood or local scale land surface model that simulates surface energy balance fluxes. However, SUEWS additionally includes vegetation, and has options for running more rapid empirical parameterisations for several fluxes. Its meteorological forcing can be from a mesoscale model like the Weather Research and Forecasting model (WRF) (Sun et al., 2024) or from reanalysis data (e.g. ERA5, Hersbach et al., 2020)(Kokkonen et al., 2018).

Traditionally, SUEWS has been used for urban surface energy flux analysis for neighbourhood climate related studies (Ao et al., 2018; Lindberg et al., 2018; Ward & Grimmond, 2017). Recent SUEWS' developments permit vertical profiles of local-scale (i.e. horizontally averaged) climatic variables within the roughness sublayer (Tang et al., 2021) to be used to assess building energy use with urban-to-building one-way coupling (Xie et al., 2023b). SUEWS is computationally cost-effective when coupled with EnergyPlus for multi-scale modelling (Xie et al., 2023b). Even when running offline (e.g. not coupled to WRF), SUEWS provides reasonable accuracy and has been widely used and evaluated in numerous global climates (see Lindberg et al. (2018) for their Table 3; Sun and Grimmond (2019) for their Table 1). Compared to WRF+BEP/BEM, the SUEWS-EnergyPlus modelling approach is more suitable for quick analysis focused on the specific neighbourhoods, requiring detailed building energy simulations over a longer period of time, which are crucial for the accurate assessment of ASHPs in residential settings. However, the two-way feedback between buildings and the local climate has not yet been considered in this context.

To address the gap in UK studies and to introduce a simpler but specific modelling approach focused on local-scale effects, we propose a two-way coupling between SUEWS and EnergyPlus to investigate the localised air temperature effects resulting from the widespread implementation of air-source heat pumps (ASHPs) in UK residential neighbourhoods under future climate scenarios. Our objectives are: (1) to quantify the potential changes in local-scale air temperatures attributable to ASHP adoption in two idealised UK residential neighbourhoods; (2) to assess how different assumptions about anthropogenic heat emissions from ASHPs affect these temperature projections; and (3) to explore the varying impacts of ASHP implementation across different UK climate zones.

2. Methods

In this study, we couple the local-scale land surface model Surface Urban Energy and Water Balance Scheme (SUEWS,SuPy v2023.7.3) (Järvi et al., 2011; Sun & Grimmond, 2019; Ward & Grimmond, 2017) and the building energy simulation tool EnergyPlus v9.4 (U.S. Department of Energy, 2020b).

2.1. Neighbourhood-scale climate modelling

The SUEWS surface energy balance is written as (Ward et al., 2016):

$$Q^* + Q_F = Q_H + Q_E + \Delta Q_S \quad (1)$$

where Q^* is the net all-wave radiation, Q_F is the total anthropogenic heat flux, Q_H is the turbulent sensible heat flux, Q_E is the latent heat flux and ΔQ_S is the net storage heat flux.

Q_F comprises heat emissions from metabolism, buildings, and transport (Grimmond, 1992). Here, we focus on heat emissions from buildings ($Q_{F,B}$), including that generated by occupants metabolism and equipment within the buildings. Building energy use is the greatest source of Q_F, contributing to around 79 % of the total in London (Ward & Grimmond, 2017). Given our focus on the relative differences between different building setups, we simplify the model by assuming the other non-building anthropogenic heat components (e.g. from outdoor human metabolism and transportation) are 0 W m^{-2} (i.e. $Q_F = Q_{F,B}$).

In SUEWS, we use the Sailor and Vasireddy's (2006) option to calculate daily mean Q_F (Sun & Grimmond, 2019), as follows:

$$Q_F = \rho_{pop}[a_{F0} + a_{F1}CDD + a_{F2}HDD] \quad (2)$$

where ρ_{pop} is the population density. The a_{F0} coefficient provides the base Q_F value from all sources at a comfort temperature (per ρ_{pop}). The a_{F1} and a_{F2} coefficients give the response to cooling degree days (CDD) and heating degree days (HDD) respectively, enabling modelled Q_F to vary with temperature and changing cooling or heating demand. Two base temperatures ($T_{b,cooling}$ and $T_{b,heating}$) are required to calculate CDD and HDD. The hourly variations are obtained using diurnal profiles obtained from EnergyPlus modelling (Section 2.2) as a model input with the daily mean obtained from Eq. (2).

The Eq. (2) coefficients can be estimated by multiple ways. Conventional, energy consumption data at city or sub-city scales are used to derive these coefficients (Ao et al., 2018). For example, in different London boroughs weekdays values vary between $a_{F0} = 0.1134$ to 0.2281 W m^{-2} (cap $ha^{-1})^{-1}$, $a_{F1} = 0$ W m^{-2} (cap $ha^{-1})^{-1}$, and $a_{F2} = 0.0038$ to 0.0076 W m^{-2} (cap $ha^{-1})^{-1}$, and for weekends $a_{F0} = 0.1073$ to 0.2119 W m^{-2} (cap $ha^{-1})^{-1}$, $a_{F1} = 0$ W m^{-2} (cap $ha^{-1})^{-1}$, and $a_{F2} = 0.0034$ to 0.0069 W m^{-2} (cap $ha^{-1})^{-1}$ (Ward & Grimmond, 2017), based on average Q_F data modelled with GreaterQF for the years 2005 to 2008 (Iamarino et al., 2012). With UK air-conditioning use currently low (Abela et al., 2016), no increase in Q_F is evident with warmer temperatures, so a_{F1} is set to zero (Kotthaus & Grimmond, 2014; Ward & Grimmond, 2017). However, with installation of air source heat pumps, the a_{F1} coefficient related to building cooling will need to be modified for the different system types and neighbourhood settings. Here we use EnergyPlus simulations of neighbourhood buildings to determine these coefficients using outdoor 2 m above ground level air temperature (T_2) for HDD and CDD calculations, consistent with typical meteorological observations and building simulations.

In SUEWS, a modified Monin–Obukhov similarity theory (MOST) approach-based roughness-sublayer module (SUEWS-RSL) is used to model the vertical profiles of air temperature, wind speed and specific humidity within the roughness sublayer (Tang et al., 2021; Theeuwes et al., 2019). Air temperature at different heights within the canopy layer is calculated as follows:

$$T(z) = T(z_h) - \frac{Q_H}{u^*\rho c_p}\frac{P_r}{\beta f}\left[1 - exp\left(\frac{\beta f(z - z_h)}{l_M}\right)\right] \quad (3)$$

where z is the height; z_h is the urban canopy layer height assumed here to be the mean building height; u^* friction velocity, ρ density of air, c_p the specific heat of air at constant pressure, P_r the Prandtl number, and l_M the mixing length. β and f are the Harman and Finnigan (2008) parameters. In SUEWS, Q_H is determined as the residual of the energy balance equation (Eq. (1)) (Ward et al., 2016). Since Q_F is an independent input, any variation in Q_F will be directly reflected on Q_H, and consequently, $T(z)$.

In SUEWS, the neighbourhood-scale net heat storage flux ΔQ_S in Eq. (1) is determined using the objective hysteresis model (OHM) (Grimmond & Oke, 1999):

$$\Delta Q_s = \sum_i f_i\left[a_{1i}Q^* + a_{2i}\frac{\partial Q^*}{\partial t} + a_{3i}\right] \quad (4)$$

where f is the surface cover fraction for each surface type, and t is time. The OHM coefficients a_1, a_2, and a_3 are typically determined from model

simulations (Arnfield & Grimmond, 1998; Meyn & Oke, 2009) or directly from observations (Ward et al., 2016). In this study we assume for simplicity the simulated neighbourhood only consists of buildings and grass. The building related coefficients are derived from EnergyPlus simulation results (Table S1) and the grass parameters are derived from observations (Omidvar et al., 2022).

The SUEWS-RSL performance for modelling local-scale climate variables has been evaluated in multiple locations. Tang et al. (2021) assess the vertical temperature profile with six months observations undertaken in central London site at two heights (12.5 m and 6.5 m above ground level). The simulated 30-min air temperatures have mean absolute errors (MAEs) of 0.59 °C (at 12.5 m) and 0.93 °C (at 6.5 m). The median diurnal cycles and interquartile ranges are consistent with observed values. The mean biased errors (MBEs) of −0.57 °C at 12.5 m and −0.93 °C at 6.5 m indicate that the simulated air temperatures are slightly underestimated at both heights. Theeuwes et al. (2019) evaluate the RSL model using vertical profiles of wind speed observations in Basel and Gothenburg, and find the model aligns well with observations, particularly when flow is over flat roofs, with MAEs ranging from 0.15 to 0.5 m s^{-1}.

2.2. Anthropogenic heat from buildings

In this study, the detailed anthropogenic heat emission from buildings $Q_{F,B}$ is calculated with EnergyPlus following Liu et al.'s (2022) approach.

When the ASHP runs in cooling/heating mode, the relation between the cooling/heating load ($Q_{cooling/heating}$, W m^{-2}) and energy consumption (Q_{EC}, W m^{-2}) is captured by the coefficient of performance (COP):

$$COP = \frac{Q_{cooling/heating}}{Q_{EC}} \tag{5}$$

The anthropogenic heat emissions from buildings (hereafter $Q_{F,B}$) represents the heat emitted to the outdoors due to human activities inside the building (Fig. 1). It is calculated as the difference in total building heat emissions between occupied (***o*** in Fig. 1) and vacant (or unoccupied, ***uo*** in Fig. 1) buildings, since even unoccupied buildings influence the local climate. This is expressed as the sum of waste heat (Q_{waste}), difference in net longwave radiation exchange between occupied and unoccupied conditions ($\Delta Q_{LW,o\text{-}uo}$), difference in convective heat exchange between occupied and unoccupied conditions ($\Delta Q_{H,o\text{-}uo}$), and difference in heat exchange through air exchange between occupied and unoccupied conditions ($\Delta Q_{AE,o\text{-}uo}$) (Liu et al., 2022):

$$Q_{F,B} = Q_{waste} + \Delta Q_{LW,o-uo} + \Delta Q_{H,o-uo} + \Delta Q_{AE,o-uo} \tag{6}$$

It can also be expressed as the sum of building internal heat gains ($Q_{internal}$) and energy consumption of heating/cooling system (Q_{EC}) minus the net building heat storage difference between occupied and unoccupied conditions ($\Delta Q_{S,o\text{-}uo}$) (Liu et al., 2022):

$$Q_{F,B} = Q_{internal} + Q_{EC} - \Delta Q_{S,o-uo} \tag{7}$$

Details on the derivation of the equations and explanations can be found in Liu et al. (2022).

To assess the impact of replacing gas boilers with heat pumps on outdoor local climate in line with current UK policy, two systems are considered: a heat pump serving both cooling and heating functions representing the future scenario, and the current prevalent gas boiler system used for heating and no active cooling for summer, considering only infiltration. The traditional gas boiler is assumed to operate with a consistent efficiency of 0.8 (Morales Sandoval et al., 2023). ASHP's COP for cooling depends on outdoor air temperature (assumed here to be the air temperature at 2 m above ground level, T_2), with a linear relation typically derived from CIBSE AM16 (CIBSE, 2021) for the UK scenario:

$$COP_{cooling} = -0.14T_2 + 7.31 \tag{8}$$

Similarly for heating:

$$COP_{heating} = 0.07T_2 + 3.20 \tag{9}$$

$Q_{F,B}$ modelled by EnergyPlus is then used in SUEWS for local climate modelling.

2.3. Feedback between T_2 and Q_F

The feedback between building energy consumption and outdoor air temperature when ASHPs are used is well known (Kikegawa et al., 2022). When providing cooling, ASHPs or air conditioners transfer heat from indoor spaces to the outside, which subsequently raises the outdoor air temperature. This temperature increase, in turn, elevates the building's cooling demand, leading to additional heat emission. The opposite occurs when ASHPs are used for heating. This feedback is accounted for in the SUEWS-EnergyPlus modelling scheme.

Iterative modelling of both $Q_{F,B}$ and local 2 m outdoor air

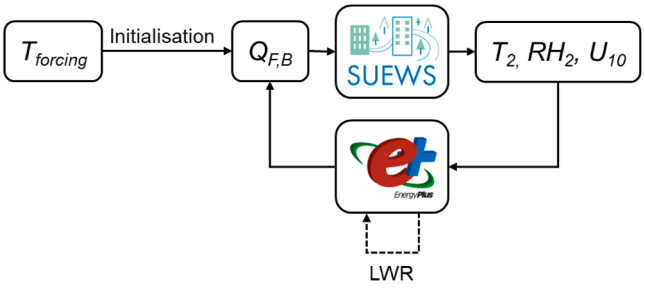

Fig. 2. Model workflow showing the feedback loop between building heat emissions $Q_{F,B}$ and outdoor air temperature T_2. LWR: inter-building longwave radiation modelling (Xie et al., 2022).

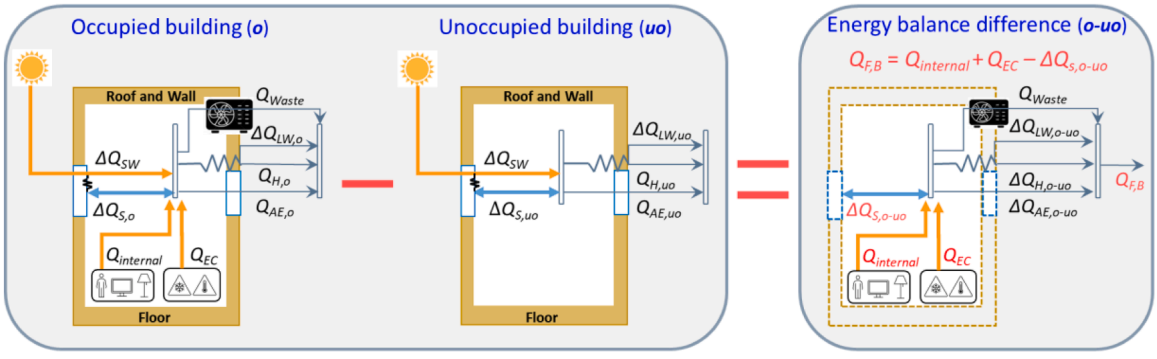

Fig. 1. Schematic of principles used to derive anthropogenic heat emission from buildings ($Q_{F,B}$) by considering the differences in heat fluxes between an 'occupied' (o) and 'unoccupied' building (uo). Modified from Liu et al. (2022).

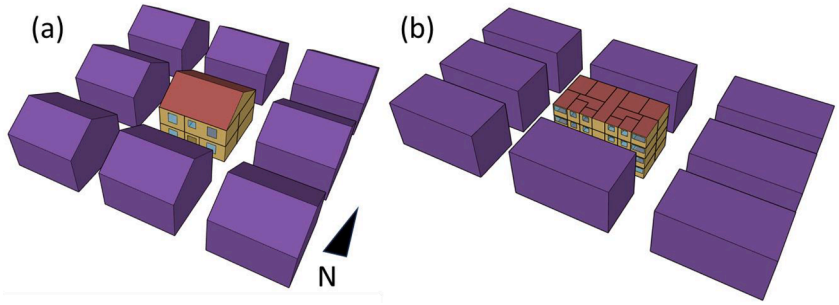

Fig. 3. Idealised neighbourhoods with a plan area fraction of 0.5 are modelled with building archetypes of: (a) detached house and (b) flats. As buildings are assumed to be in a neighbourhood rather than isolated, the impacts of these interactions are accounted for.

temperature (T_2) captures these feedbacks (Fig. 2). An initial $Q_{F,B}$ is obtained using HDD and CDD calculated using the initial forcing air temperature $T_{forcing}$ for SUEWS, to obtain a modified T_2. Thereafter, this T_2 is used to calculate a new $Q_{F,B}$ via EnergyPlus simulations, which also have internal iterations to ensure inter-building longwave radiation (Fig. 2) is accounted for (Xie et al., 2022).

The updated $Q_{F,B}$ is used in SUEWS to update T_2. This whole procedure continues until the difference in T_2 between successive iterations is consistently less than a tolerance value of 0.01 °C. In this study, only three iterations are needed. Given small computational time needed per iteration (< 2 min), two-way coupling remains time-efficient. By accounting for the feedbacks, the $Q_{F,B}$ difference predicted (gas boiler to ASHP) is improved by 14 % in median on a typical hot day (Fig. S1).

Although SUEWS-EnergyPlus is two-way coupled, it is an offline or sequential coupling with an exchange of the annual time series data. Sequential coupling has the benefits of numerical stability and less computational demands (cf. direct coupling at each timestep). Some feedback will be missed but the benefits of fast, numerically stable, long-term simulations outweigh this drawback.

2.4. Building energy simulation

Given the UK government's recent measures and policies that provide financial aid to replace fossil fuel heating systems with heat pumps in UK homes (Department for Energy Security & Net Zero, 2023), here we focus on residential buildings.

Two UK building archetypes are considered here: detached house archetype (Fig. 3a) with length (L) of 8.8 m, width (W) of 8.5 m and height (H) of 7.5 m; and low-rise flat building archetype (Fig. 3b) with 18.1 m × 9.5 m × 10 m ($L \times W \times H$). In England, these two archetypes constitute the primary types of private owner-occupied (24 %) and social (37 %) dwellings, respectively (Department for Communities & Local Government, 2013). Additionally, they represent the main archetypes in rural (42 %) and urban (28 %) areas in England respectively (Office for National Statistics, 2023). The buildings' geometry and construction parameters are characterised based on Porritt (2012) and Liu (2017), as of with post-1996 well-insulated cavity brick walls (Table 2).

To maximise the use of ASHP, we assume the occupancy to be two elderly people whose behaviour is to stay at home throughout the day but move between different rooms (for the detailed schedule, see Porritt (2012), Table 3.6). The appliances include a TV (150 W) and a fridge (50 W) (see Porritt (2012), Table 3.7). The heating and cooling set points are

Table 3
Coefficients for SUEWS Q_F calculation (Eq. (2)). See also Fig. 5.

	Detached house		Flat	
	ASHP	Gas boiler	ASHP	Gas boiler
a_{F0} (base) [W m^{-2} (cap ha^{-1})$^{-1}$]	0.0270	0.0281	0.0280	0.0282
a_{F1} (cooling) [W m^{-2} (cap ha^{-1})$^{-1}$]	0.0035	0	0.0026	0
a_{F2} (heating) [W m^{-2} (cap ha^{-1})$^{-1}$]	0.0009	0.0037	0.0004	0.0018
$T_{b,\ heating}$ (°C)	17.4	16.0	16.6	15.2
$T_{b,\ cooling}$ (°C)	20.4	–	20.1	–

Table 2
Construction and thermal characteristics (Liu, 2017; Porritt, 2012) of detached houses and flats modelled. SHGC: solar heat gain coefficient. The corresponding OHM coefficients (Eq. (4)) for SUEWS heat storage calculation are in Table S1.

	Construction	U-value (W m^{-2} K)
External wall (Insulated cavity wall)	• 105 mm brickwork outer leaf • 100 mm air layer (Air gap>25 mm) • 50 mm EPS Expanded Polystyrene (Standard) • 105 mm brick, inner leaf • 13 mm plaster (dense)	0.5
Internal partition	• 15 mm gypsum plasterboard • 50 mm air layer • 15 mm gypsum plasterboard	1.79
Internal floor	• 10 mm plasterboard (ceiling) • 200 mm air layer • 20 mm timber flooring • 5 mm carpet/textile flooring	1.33
Ground floor	• 50 mm EPS Expanded Polystyrene • 150 mm concrete roof/floor slab • 50 mm flooring screed	0.5
Roof	• 10 mm concrete roof tiles • 250 mm min wool quilt • 10 mm plasterboard (ceiling)	0.16
Doors	• 35 mm oak	2.25
Windows	• 6 mm generic clear glass • 13 mm air • 6 mm generic clear glass	2.71, SHGC = 0.7

20 and 24 °C, respectively (Wang et al., 2009). In scenarios when heating or cooling systems are operational, it is assumed windows remain closed, with an infiltration rate of 0.5 ACH (Porritt, 2012).

An idealised neighbourhood typified by homogenous buildings that collectively occupy 50 % of the plan area is considered here, consistent with a fairly dense UK residential setting (Ward & Grimmond, 2017), assuming expected trends in urban densification. This results in 134 people per hectare for the neighbourhood with detached houses (2 people per building) and 435 people per hectare for the neighbourhood with flats (16 people per building). For the neighbourhood-building coupled simulation, an iterative approach is used to consider long-wave radiative components (Fig. 1) (Xie et al., 2022) and wind pressure coefficient of the target building is modified (Xie et al., 2023a).

2.5. Weather data

To assess the extreme buildings anthropogenic heat emissions, the Design Summer Year (DSY) is used, which is the year with the 3rd warmest non-heating months (April to September) in 20 years (CIBSE, 2014). Simulations using two periods are compared: (1) the recent past 1980–1999 (hereafter 1990s) and (2) a future 2040–2059 period (hereafter 2050s) (Section 3.4). These are derived by Eames et al. (2011) from the UK Climate Projections (UKCP09) (DERFA, 2009). For the 2050s the medium emissions scenario is used, which aligns with the IPCC A1B scenario assuming balanced use of fossil fuels and non-fossil fuels (WMO, 2000).

Despite having a warm summer, the DSY weather data show similar winter air temperatures (mean ± standard deviation (°C): 7.41±3.38) as the Test Reference Year (TRY) weather data (7.36± 4.01 °C), which represents a typical year. Therefore, winter conditions in the DSY are considered representative of typical conditions.

Modelling is undertaken for nine cities spread across the UK (Fig. 4c). The 2050s DSY mean summer air temperatures are 2 °C (Aberdeen) to 3.7 °C (Plymouth) higher than the 1990s (Fig. 4a cf. 2b). London is projected to have the warmest summer temperatures (20.3 °C).

2.6. Comparison scenarios

Building anthropogenic heat emissions ($Q_{F,B}$) associated with the use of ASHPs are calculated assuming:

Waste heat Q_{waste} versus $Q_{F,B}$:

Conventionally the waste heat emission (Q_{waste}) from the air conditioner has been widely used to approximate the anthropogenic heat emission from buildings (Sailor, 2011) (see Table 1). Q_{waste} is calculated by summing cooling load ($Q_{cooling}$) and cooling system energy consumption accounting for the system COP:

$$Q_{waste} = Q_{cooling} \times \left(1 + COP_{cooling}^{-1}\right) \quad (10)$$

However, Q_{waste} only considers the heat emitted by the air conditioning system itself, neglecting variations in storage heat flux resulting from human activities which impact building's heat emissions to the outdoor environment. This oversight could lead to biases in building heat emissions in summer, as indicated by Liu et al. (2022). These biases are analysed in Section 3.2.

All rooms versus occupied rooms:

Assuming all areas are heated/air-conditioned (Wang et al., 2018) differs from the more cost-effective practice of not using heating/cooling in unoccupied rooms (Abela et al., 2016; Soebarto & Bennetts, 2014; Yan et al., 2015). It is assumed ASHP operation occurs: (a) in occupied rooms only, representing an efficient use of energy and minimising $Q_{F,B}$ while ensuring indoor temperature control for occupants; and (b) throughout the entire building, which represents a less efficient, pessimistic case of energy use and maximises $Q_{F,B}$. The two scenarios are compared in Section 3.3.

3. Results

3.1. London base case for 2050s climate projection

The 2050s annual average building anthropogenic heat emissions ($Q_{F,B}$) of detached houses with gas boilers is 6.6 W m^{-2} (Fig. 5a) whereas for flats it is 17.6 W m^{-2}. These values are reasonable for the range of values across all domestic settings in Greater London of 1.1 to 36.5 W m^{-2} for the 2005 to 2008 period (Iamarino et al., 2012), with the largest values associated with more densely built non-residential areas than simulated here.

During the heating season (October to April), the $Q_{F,B}$ for gas boiler cases typically exceed those of ASHPs (Fig. 5a, b, red cf. black) due to the gas boiler's lower efficiency (COP of 0.8) in contrast to that of the ASHP (COP of 3 to 4.5). The peak winter hourly $Q_{F,B}$ for detached house neighbourhoods with gas boilers reaches 16.2 W m^{-2} and 45.2 W m^{-2} for flats. These are reduced in both neighbourhoods when replaced with ASHPs (8.6 W m^{-2} and 31.9 W m^{-2}, respectively). In the warmer months of May to September, the diurnal $Q_{F,B}$ range for gas boiler neighbourhoods remains relatively constant, with values up to 6.1 W m^{-2} for detached houses and 25.3 W m^{-2} for flats (Fig. 5a, b, red cf. black). The neighbourhoods with ASHP have higher $Q_{F,B}$ values during these months as the AHSP can provide cooling, with hourly peaks reaching 11.6 W m^{-2} (detached) and 39.6 W m^{-2} (flats).

When analysing the anthropogenic heat flux emission normalized by population density ($Q_{F,B}/\rho_{pop}$) alongside the mean daily 2 m outdoor air

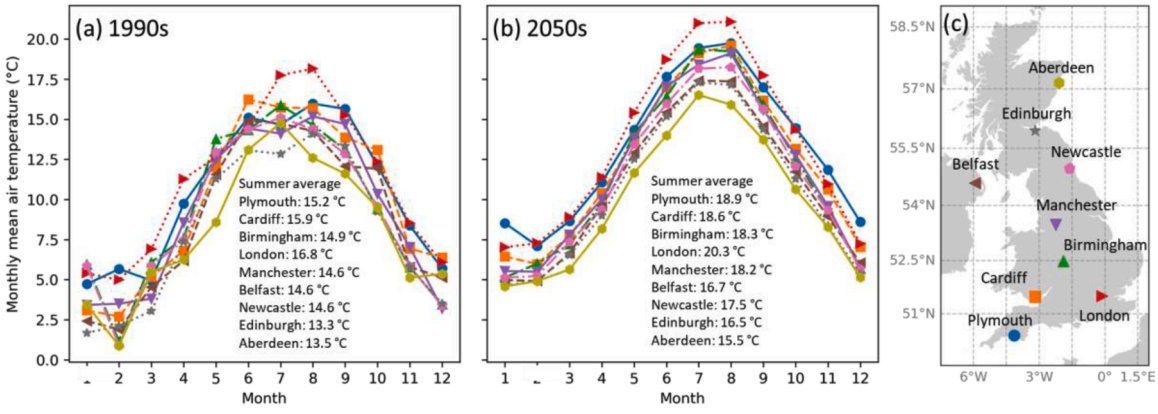

Fig. 4. UKCP09 design summer year (DSY) monthly mean air temperature (Eames et al., 2011) for: (a) 1990s and (b) 2050s, across (c) different UK cities.

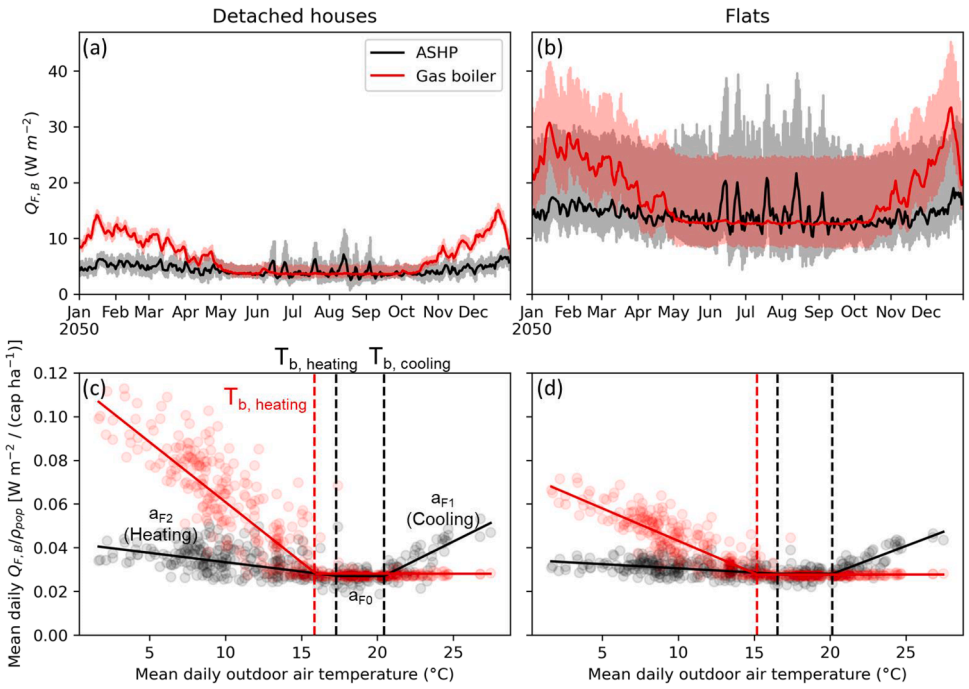

Fig. 5. London 2050s design summer year EnergyPlus simulated daily mean (lines) and hourly (shading) building anthropogenic heat flux ($Q_{F,B}$) with air-source heat pumps (ASHP) and gas boiler for (a) detached houses and (b) flats; and (c, d) normalised by population density (ρ_{pop}) and the relation mean neighbourhood (columns, Fig. 3) daily 2 m outdoor air temperature for different with Eq. (2) coefficients (Table 3). T_b are the base temperatures used in the cooling/heating degree days calculation.

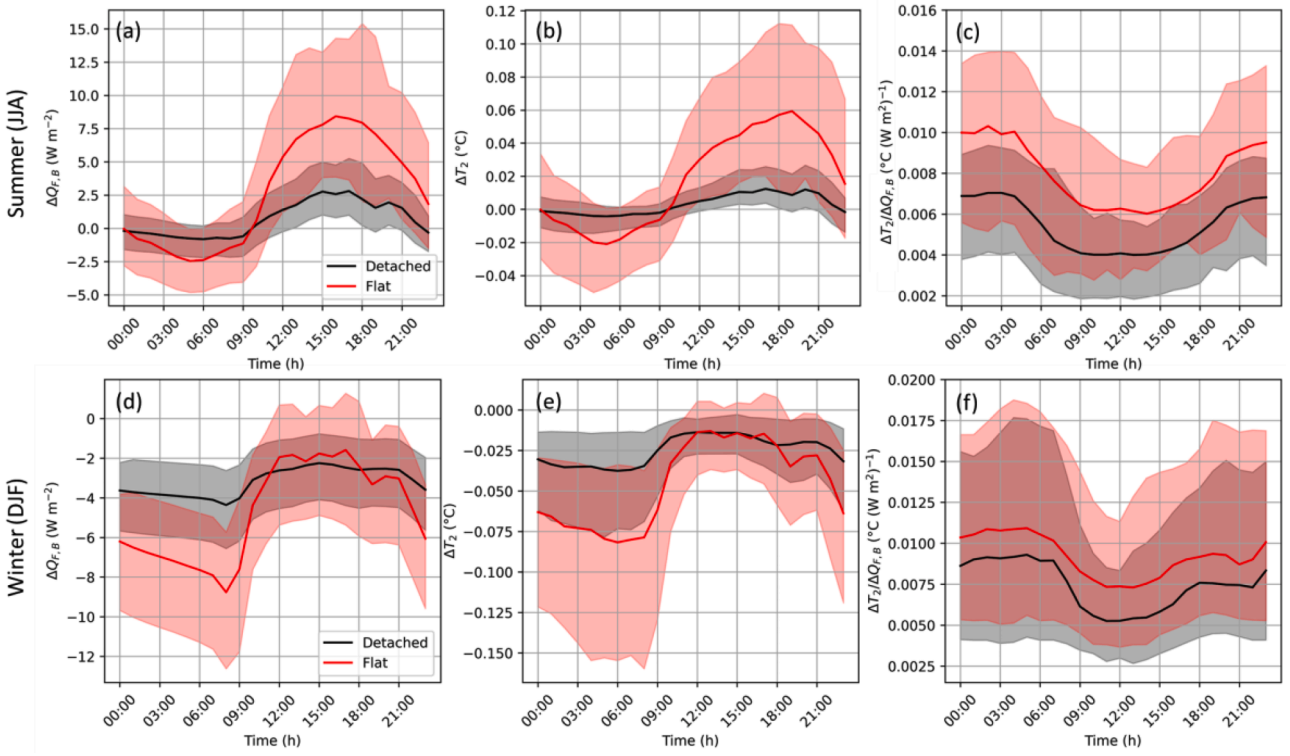

Fig. 6. London 2050s summer (JJA) and winter (DJF) building archetype neighbourhoods (colour) median (line) and 5th and 95th percentiles (shading) difference between those with air-source heat pumps (ASHP) and gas boiler installed impact on: (a, d) anthropogenic heat emission ($\Delta Q_{F,B}$), (b, e) 2 m air temperature (ΔT_2), and (c, f) ΔT_2 to $\Delta Q_{F,B}$ ratio. Note Y-scale differs between seasons (rows).

temperature (Fig. 5c, d), ASHP neighbourhoods display the characteristic U-shaped curve similar to cities with notable heating and cooling needs, like Shanghai (Ao et al., 2018). The left and right segments slopes represent a_{F2} and a_{F1} for Eq. (2), and the horizontal segment represents a_{F0} (Table 3). Although the flats have overall larger $Q_{F,B}$, their a_{F1} and a_{F2} are lower compared to detached houses due to higher population densities and smaller cooling/heating area per person. The heating coefficients derived here are slightly smaller than current London

boroughs estimates (0.0039 to 0.0076 W m^{-2} (cap ha^{-1})$^{-1}$; Ward & Grimmond, 2017), possibly due to different building types (residential and non-residential), population density and traffic, and diverse heating system efficiencies.

The impact of ASHP-wide neighbourhood usage relative to the traditional gas boiler usage on the outdoor summer 2 m air temperature (T_2) is assessed using SUEWS with the updated heat storage coefficients (Table S1) and diurnal $Q_{F,B}$ profiles (Section 2.1), as shown in Fig. 6. This impacts the diurnal patterns of $Q_{F,B}$ and T_2. Adoption of ASHPs for cooling can increase daytime $Q_{F,B}$, while potentially reducing nighttime $Q_{F,B}$ (Fig. 6a) due to decreased heat storage in the building envelope as a result of lower indoor temperatures during the day. Consequently, ASHP usage could mitigate nocturnal urban heat island effects, particularly during periods when cooling is unnecessary. The median increase in daily peak $Q_{F,B}$ is 2.5 W m^{-2} for detached houses and 8.4 W m^{-2} for flats (Fig. 6a), leading to T_2 increases of approximately 0.01 °C and 0.06 °C (Fig. 6b), respectively. These results suggest that the contribution to overheating by ASHP adoption in the studied low-rise residential neighbourhood is small.

On a typical hot day, with forcing air temperatures reaching 32 °C, the peak $Q_{F,B}$ increase is 6.4 W m^{-2} for detached houses and 19.3 W m^{-2} for flats (Fig. 7a), leading to T_2 peak increases of 0.03 °C and 0.12 °C (Fig. 7b), respectively. With warmer outdoor T_2 increasing cooling demand, the nighttime $Q_{F,B}$ associated with ASHP use is larger than that with gas boiler use (Fig. 7a).

In winter, ASHPs absorb heat from the outdoors providing indoor heating, resulting in lower anthropogenic heat emissions compared to gas boilers. Replacing gas boilers with ASHPs can reduce $Q_{F,B}$ by 4.4 W m^{-2} for detached houses and 8.8 W m^{-2} for flats when outdoor air temperature T_2 is the lowest (Fig. 6d), leading to daily minimum T_2 reduction of 0.03 °C and 0.08 °C, respectively (Fig. 5e). On a typical cold day with a minimum air temperature of −1.7 °C, $Q_{F,B}$ can be reduced by 5.6 W m^{-2} for detached houses and 11.1 W m^{-2} for flats (Fig. 7d), resulting in a decrease in daily minimum T_2 of up to 0.08 °C and 0.16 °C (Fig. 7e), respectively. Such decreases in outdoor air temperature could potentially lead to a slight increase in building heating loads, although the impact remains small in the studied neighbourhoods.

The local scale feedback can be assessed by calculating the ratio of the temperature response (ΔT_2) to the change in anthropogenic heat flux (ASHP cf. gas boiler) ($\Delta Q_{F,B}$) (Wang et al., 2023). The ratio tends to be higher at night and lower during the day (Fig. 6c, f), consistent with others' findings (Takane et al., 2019). Based on Eq. (3), this ratio mainly depends on $\frac{1}{u^* \beta f}\left[1 - \exp\left(\frac{\beta f (z - z_h)}{l_M}\right)\right]$. As the diurnal variations of β, f and l_M are small, the diurnal pattern mainly depends on friction velocity u^* which is larger during unstable conditions and smaller under stable conditions. Typically unstable conditions occur more during the day and stable conditions occur more at night, so the $\Delta T_2/\Delta Q_{F,B}$ ratio has the inverse pattern (Kotthaus & Grimmond, 2014; Rigden et al., 2018). The summer median ΔT_2 response to $\Delta Q_{F,B}$ varies through the day from 0.004 to 0.007 °C (W m^{-2})$^{-1}$ for detached houses and 0.006 to 0.010 °C (W m^{-2})$^{-1}$ for flats (Fig. 6c). On a typical hot day (Fig. 7c), these values are slightly less than the median (Fig. 6c), varying between 0.004 and 0.007 °C (W m^{-2})$^{-1}$ for detached houses and 0.005 to 0.009 °C (W m^{-2})$^{-1}$ for flats. In winter, due to generally more stable conditions, the median $\Delta T_2/\Delta Q_{F,B}$ ratios can increase to 0.005 to 0.009 °C (W m^{-2})$^{-1}$ for detached houses and 0.007 to 0.011 °C (W m^{-2})$^{-1}$ for flats. On a typical cold day, these ratios can further rise to 0.006 to 0.015 °C (W m^{-2})$^{-1}$ and 0.008 to 0.017 °C (W m^{-2})$^{-1}$, respectively.

3.2. Waste heat Q_{WASTE} versus $Q_{F,B}$

In many other related studies (see Table 1), waste heat (Q_{waste}, Eq. (10)) from the air conditioner is used to represent building anthropogenic heat emission in summer. To further distinguish the difference between the two, waste heat values are used to derive the a_{F0}, a_{F1} and a_{F2} coefficients (Table S2). As only heat discharged by the active heating/cooling systems are considered here, there is no waste heat emission when the systems are inactive. Therefore, the baseline load (a_{F0}) of waste heat is typically negligible (Fig. 8).

Here we focus on the waste heat from ASHPs in summer (Fig. 8). The peak hourly waste heat emissions from detached houses with ASHPs can reach 10.9 W m^{-2} and 28.8 W m^{-2} for flats, which are slightly smaller than $Q_{F,B}$. As ASHPs extract heat from external air for heating purposes, negative waste heat emissions occur when outdoor air temperature is low in early June.

Using waste heat values may overpredict actual building anthropogenic heat increase from replacing gas boilers with ASHPs during

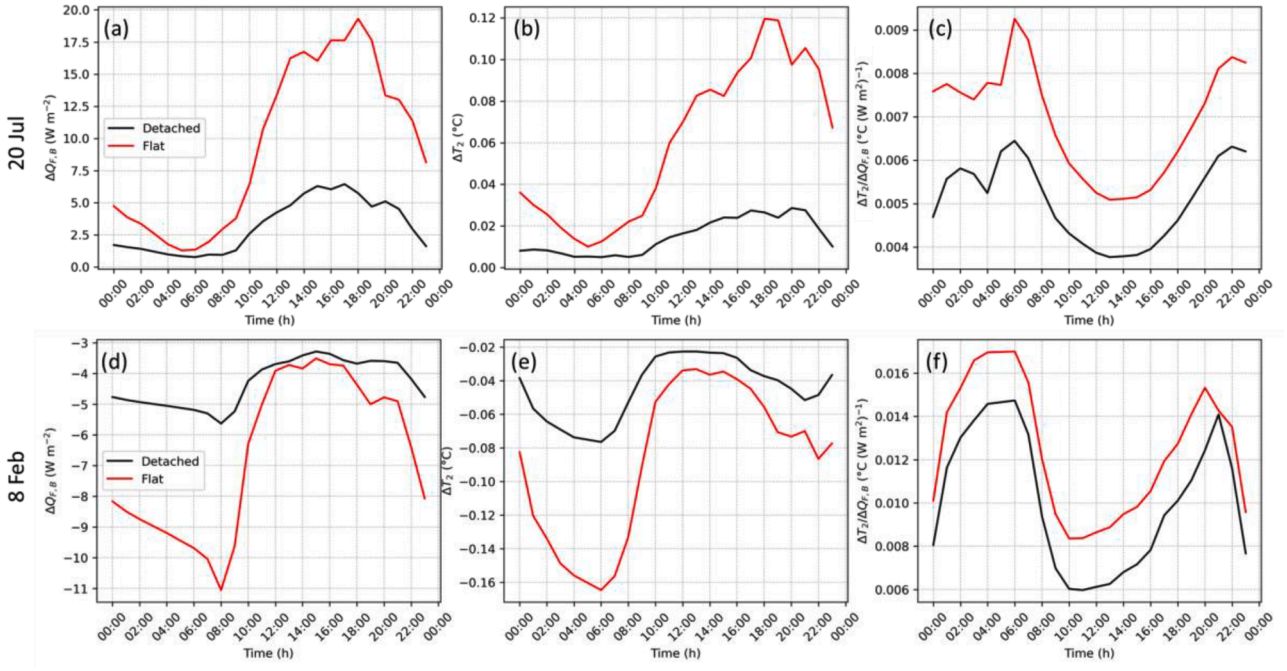

Fig. 7. As Fig. 6, but on a typical hot day (20 July) and a cold day (8 February).

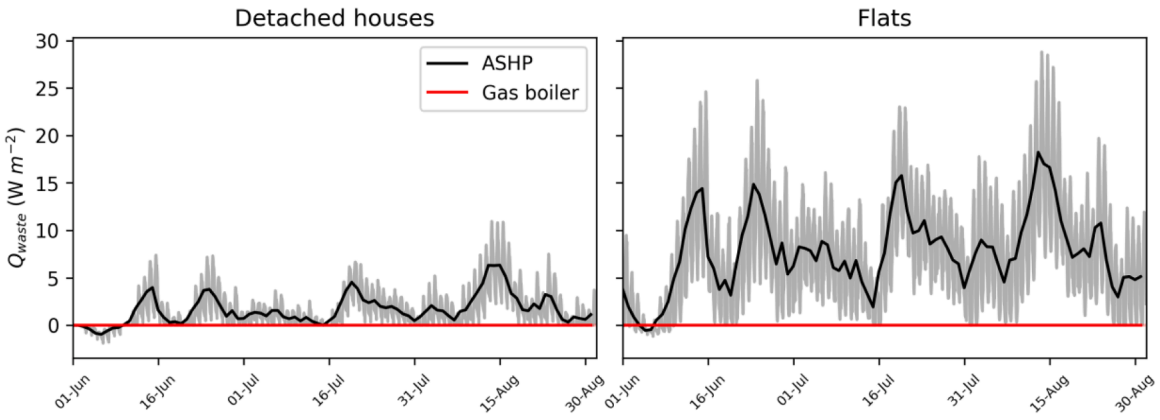

Fig. 8. As Fig. 5a, b, but for waste heat (Eq. (10)) emissions in summer (JJA).

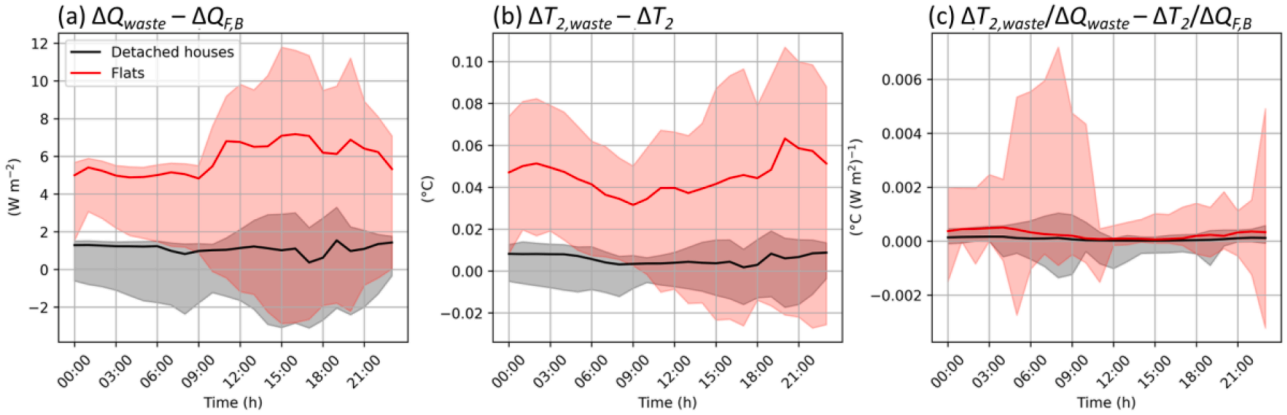

Fig. 9. As Fig. 6, but overprediction due to using waste heat as building anthropogenic heat emissions in summer (JJA).

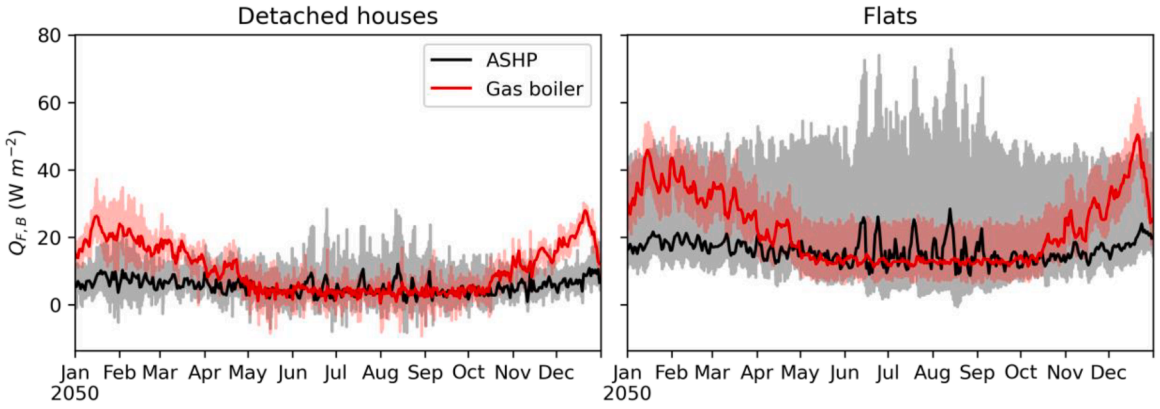

Fig. 10. As Fig. 5a, b, but with heating and cooling for all zones.

summer for detached houses (median = 1.5 W m^{-2}) by 60 % and flats (7.2 W m^{-2}) by 86 % (Fig. 9a). On a typical hot day (Fig. S2) this overprediction may be even larger (4.0 and 14.0 W m^{-2}, respectively). This results in an overpredicted median T_2 increase of 0.01 °C for detached houses and 0.06 °C for flats (Fig. 9b), or larger on hot days (0.02 and 0.12 °C, respectively). However, the sensitivity of temperature increase (ΔT_2) to anthropogenic heat flux change ($\Delta Q_{F,B}$) is only slightly overpredicted (Fig. 9c).

3.3. Impact of floor area with heating and cooling

When compared to the scenario where only occupied rooms are air-conditioned in summer (discussed in Sections 3.1 and 3.2), the scenario in which ASHPs are used to air-condition all rooms results in a notable increase in the annual mean anthropogenic heat by 23 % (to 5.4 W m^{-2}) for detached house neighbourhoods and 13 % (16.1 W m^{-2}) for those with flats (Fig. 10 cf. Fig. 5).

When looking at the diurnal variation in summer (Fig. 11a), the median overprediction of $\Delta Q_{F,B}$ increases to 1.7 W m^{-2} for detached houses and 4.5 W m^{-2} for flats, or 68 % and 54 % greater than if only the main occupied rooms are considered. A typical hot day case could have overpredictions of 5.9 W m^{-2} (detached houses) and 15.2 W m^{-2} (flats) (Fig. S3). These overpredictions in $\Delta Q_{F,B}$ may increase T_2 by a median of 0.01 °C and 0.03 °C, and by a maximum of 0.03 °C and 0.12 °C for the two types of neighbourhoods (Fig. 11b).

In winter, with larger $Q_{F,B}$ from gas boilers, the median

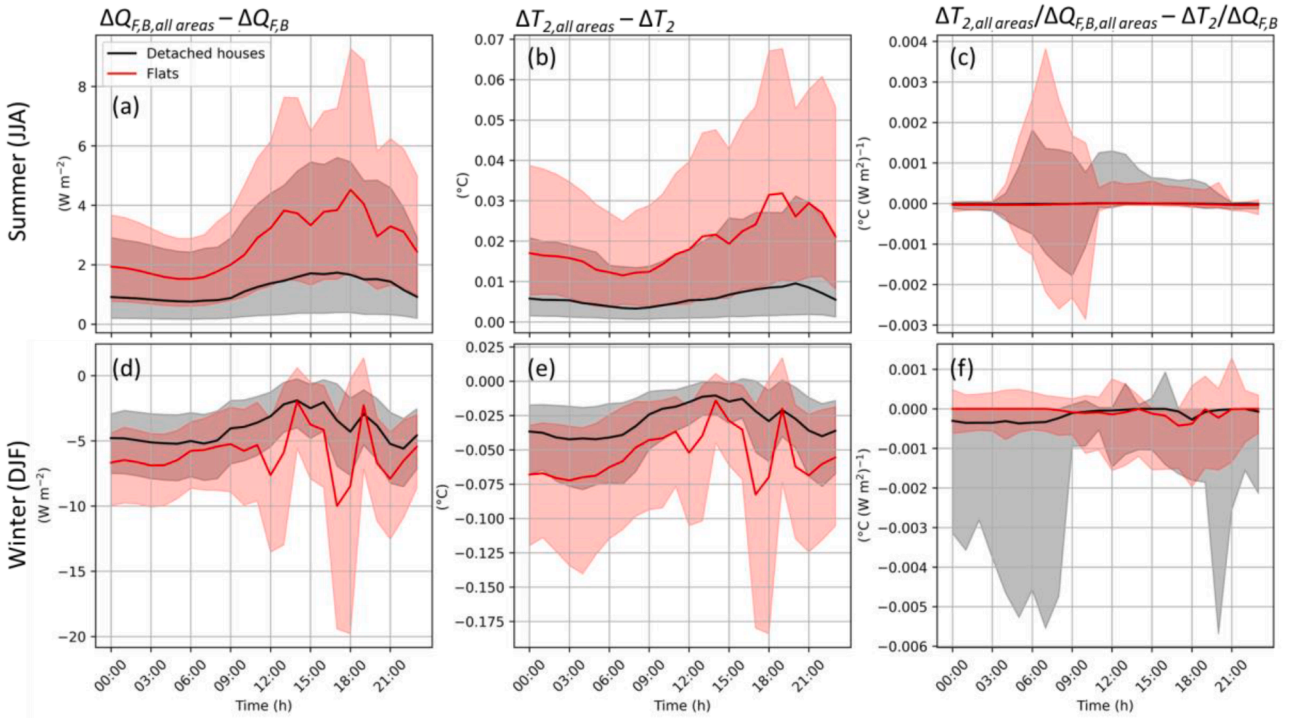

Fig. 11. As Fig. 6, but overprediction from assuming all areas are air conditioned.

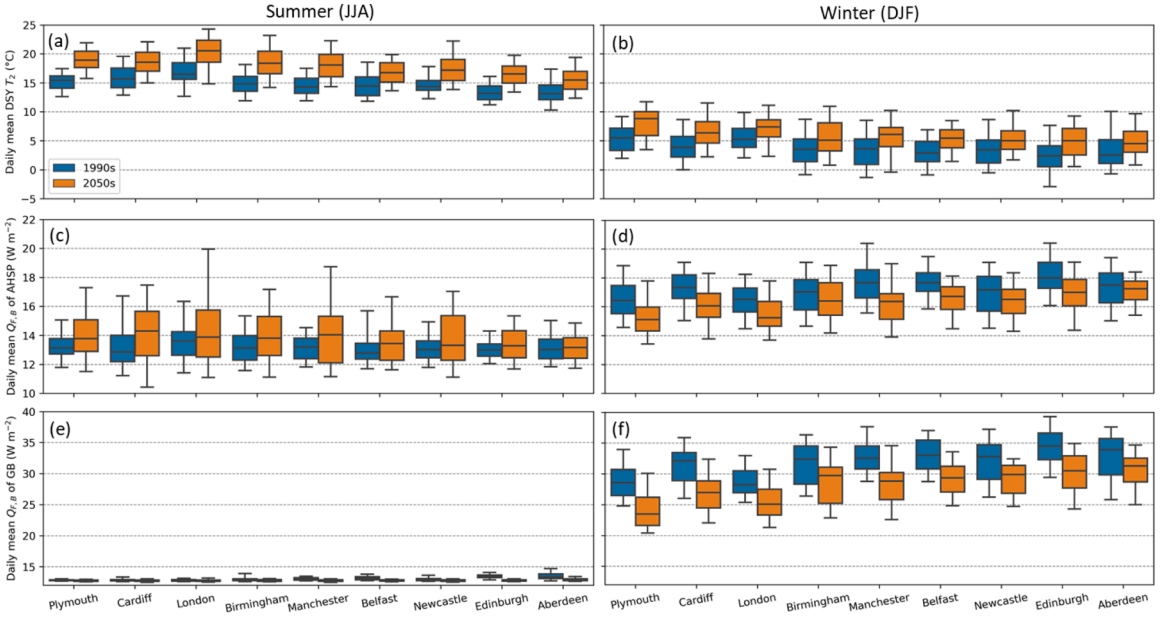

Fig. 12. For flats in UK cities (with increasing latitude, Fig. 4c) under 1990s and 2050s (colour) for (a, c, e) summer (JJA) and (b, d, f) winter (DJF) climate, the variability of the daily mean (a, b) 2 m DSY air temperature (T_2) (monthly values shown in Fig. 4a, b), (c, d) anthropogenic heat emissions ($Q_{F,B}$) from ASHP, and (e, f) $Q_{F,B}$ from gas boilers. Median (horizontal line), interquartile range (box), and 5th and 95th percentiles (whiskers) shown. London 2050s $Q_{F,B}$ results given in Fig. 5b.

overprediction of decreased $\Delta Q_{F,B}$ rises to 5.6 W m^{-2} for detached houses and 10.0 W m^{-2} for flats (Fig. 11d), or 224 % and 400 % greater than when considering only the main occupied rooms. This leads to a further overprediction of ΔT_2 reduction by 0.04 °C and 0.08 °C (Fig. 11e). Nevertheless, the ratio of ΔT_2 to $\Delta Q_{F,B}$ generally remains unchanged across both seasons, with some deviations due to atmospheric stability (Fig. 11c, f).

3.4. Impact of different UK climates for neighbourhoods with flats

Variations in UK climate result in different changes in daily mean T_2 and anthropogenic heat emissions $Q_{F,B}$ when ASHP are installed. The 2050s median daily mean T_2 is projected to be 2.3 °C (in Aberdeen) to 4.1 °C (in London) warmer than 1990s climates in summer, and 1.6 °C (Birmingham) and 3.4 °C (Plymouth) in winter (Figs. 4, 12a, b). As noted in Section 2.5, southern cities (e.g. Plymouth) are warmer than northern cites (e.g. Aberdeen) because of latitude (or earth-sun geometry).

When ASHPs are installed in flats and operate in occupied rooms

only, there is clear variability in $Q_{F,B}$ between cities (Fig. 12c, d). However, this variation does not follow a simple latitude-based pattern, as ASHPs maintain comfortable indoor temperatures (20 °C to 24 °C) for both heating and cooling provisions. The change in climates from 1990s to 2050s results in summer $Q_{F,B}$ median daily mean changes of only 0.1 W m^{-2} in Aberdeen but as high as 1.4 W m^{-2} in Cardiff and London (Fig. 12c). The latter's warmer climates have clearly higher $Q_{F,B}$ values. Despite Plymouth having the second warmest summer air temperatures (Figs. 4, 12), the coastal location in the prevailing wind direction reduces the range of temperature extremes and the median daily mean $Q_{F,B}$. Higher latitude cities (e.g. Aberdeen, Edinburgh) typically have the lowest summer $Q_{F,B}$, linked to their consistently cooler temperatures.

The winter pattern of $Q_{F,B}$ changes from the 1990s to the 2050s shows a clearer correlation with latitude (Fig. 12d). The use of ASHPs for heating decreases median daily mean $Q_{F,B}$ by 1.3 W m^{-2} in Plymouth, but only 0.3 W m^{-2} in Aberdeen. This suggests the impact of climate change on heating energy use is greater in warmer, lower-latitude cities in the UK.

The projected warmer climate of the 2050s is expected to cause greater variability in summer $Q_{F,B}$ compared to 1990s for each city (Fig. 12c). This is partly from new cooling demands being met by ASHPs, leading to emissions from both heating and cooling operations. However, with outdoor temperatures more frequently within the comfort range, particularly in cool seasons, this reduces the periods when ASHPs need to operate for heating. For example, Cardiff 5th percentile $Q_{F,B}$ (10.4 W m^{-2}) in the 2050s occurs when the mean air temperature is 15.5 °C, whereas the equivalent 1990s day is cooler (14.9 °C) but with a larger $Q_{F,B}$ (11.1 W m^{-2}).

As climate changes (1990s to 2050s), $Q_{F,B}$ from ASHP cooling will increase (Fig. 12c), but $Q_{F,B}$ from heating will decrease (Fig. 12d, F). Replacing gas boilers with ASHPs across these cities will cause changes in $Q_{F,B}$ and outdoor temperature (Fig. 13). The largest $\Delta Q_{F,B}$ occurs at around 16:00 in summer (Fig. 14a) and 8:00 in winter (Fig. 14d). These variations (Fig. 13) are impacted by the temperature changes (Fig. 12a), with larger summer differences in lower latitude cities and larger winter differences in higher latitude cities. For example, the largest change among the locations analysed occurs for London, where the summer median/maximum of the daily maximum $\Delta Q_{F,B}$ is 8.4/19.7 W m^{-2} (Fig. 13a), while in Aberdeen it is only 2.8/5.6 W m^{-2}. Conversely in winter, London's median/minimum for the daily minimum $\Delta Q_{F,B}$ is −8.8/13.3 W m^{-2}, and Aberdeen's is −14.4/20.6 W m^{-2} (Fig. 13b).

The across climates variability in ΔT_2 is consistent with the $\Delta Q_{F,B}$ pattern (Fig. 12c, d). In summer, in the warmest city (London) the median daily peak ΔT_2 is 0.06 °C (maximum of 0.13 °C), whilst Aberdeen has a more modest increase (0.02 °C median, 0.05 °C maximum). In winter, the median daily minimum ΔT_2 in London is −0.10 °C, with the largest decrease being −0.16 °C, while Aberdeen has a median of −0.14 °C and a largest of −0.23 °C.

Although some variations in ΔT_2 to $\Delta Q_{F,B}$ ratio at the time of the $\Delta Q_{F,B,peak}$ (i.e. $\Delta T_2/\Delta Q_{F,B,peak}$) occur, it remains relatively consistent across different cities, especially in summer when the atmosphere is more unstable (Fig. 13e, F). The hourly $\Delta T_2/\Delta Q_{F,B}$ ratio typically decreases during daylight hours and increases at night for all locations (Fig. 14c, F). The intra-day and day-to-day variabilities of the $\Delta T_2/\Delta Q_{F,B}$ ratio are larger than the variability between different locations. During the day, median values fluctuate around 0.002 to 0.004 °C (W m^{-2})$^{-1}$, with day-to-day variations reaching approximately 0.008 °C (W m^{-2})$^{-1}$ in summer and 0.010 °C (W m^{-2})$^{-1}$ in winter. The largest differences among locations occur under more stable atmospheric conditions (more common at night and winter), with values around 0.002 °C (W m^{-2})$^{-1}$. These findings indicate that the influence of heat emissions on air temperature is governed by a set of complex factors, rather than climate alone.

4. Discussion

Previous studies have highlighted the significant role of anthropogenic heat emissions in exacerbating urban heat island effects, specifically focusing on the influence of air-conditioning systems (Table 1) using meso-scale models with BEP/BEM that regard buildings as uniform 'shoebox' structures. Although computationally efficient and reasonably accurate compared to detailed building energy models when both use the 'shoebox' building model, BEP/BEM cannot capture the complexities of indoor-outdoor heat transfer processes in real-world building operations.

Addressing this gap, our study integrates a local-scale land surface model, SUEWS, with a detailed building energy simulation tool, EnergyPlus (Xie et al., 2023b). This novel two-way coupling between SUEWS and EnergyPlus allows for detailed simulations of representative building archetypes (detached houses and flats) and considers factors such as detailed building geometry, space types and operational patterns. This

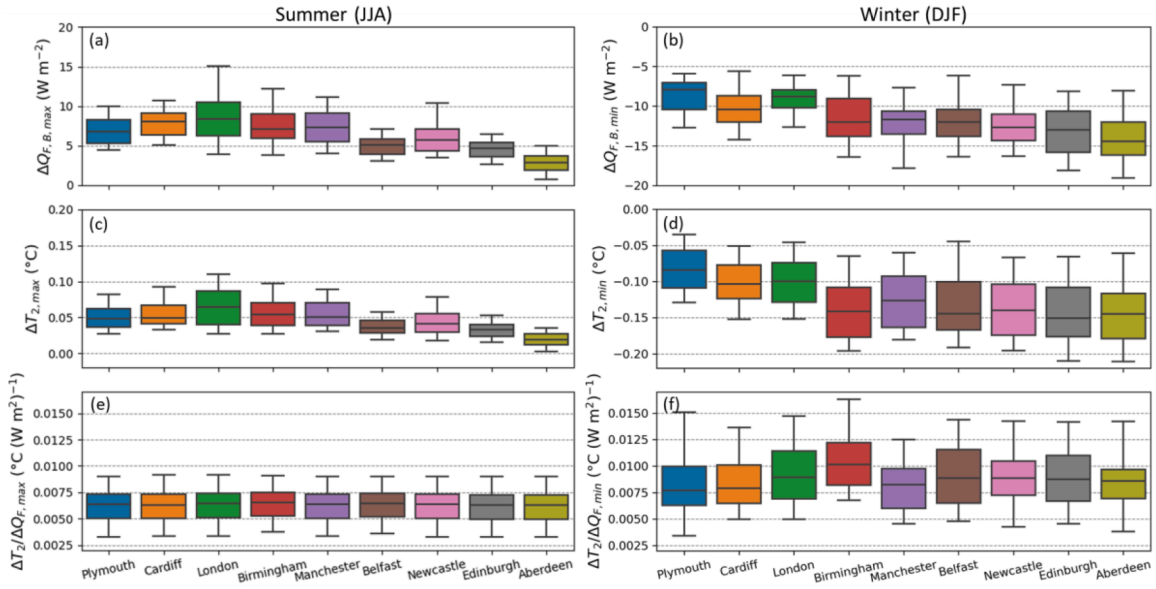

Fig. 13. As Fig. 12, but variability from replacing gas boiler with ASHPs (a, b) change in daily maximum/minimum anthropogenic heat emission ($\Delta Q_{F,B,\ max/min}$), (b) change in daily maximum/minimum 2 m air temperature (ΔT_2), and (c) ΔT_2 to $\Delta Q_{F,B}$ ratio at the time of $\Delta Q_{F,B,\ max/min}$ (i.e. $\Delta T_2/\Delta Q_{F,B,\ max/min}$), across different UK locations in 2050s.

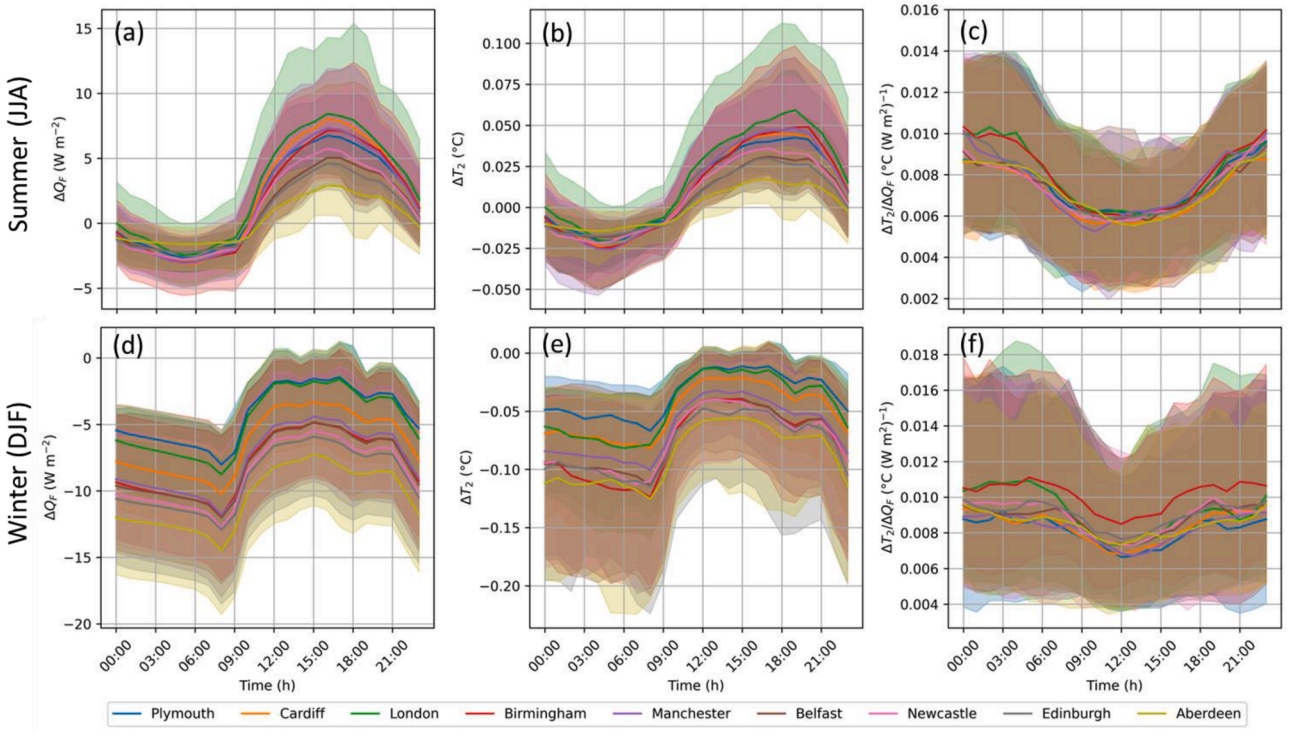

Fig. 14. Median (line) and 5th and 95th percentiles (shading) for (a) increases in anthropogenic heat emission ($\Delta Q_{F,B}$), (b) increases in 2 m air temperature (ΔT_2) and (c) $\Delta T_2/\Delta Q_{F,B}$ in summer (JJA) by replacing gas boilers with ASHPs for different UK locations in the 2050s design summer year.

approach enables a quick and specific analysis of the interplay between urban climate dynamics and building behaviour, thereby offering a detailed understanding of the thermal implications of ASHP adoption.

Our results show that for low-rise residential neighbourhoods across the UK, the increase in 2 m outdoor air temperatures from ASHP cooling is $\leq$ 0.12 °C with an increase in anthropogenic heat emission of $\leq$ 19.3 W m^{-2}. Similar air temperature increases are also reported by Brousse et al. (2024) when using WRF-BEP/BEM. They estimate the widespread (100 % of buildings) use of air conditioners during a 2018 heatwave would have increased London's average 2 m air temperature by up to 0.15 °C, but they do not indicate what the associated increase in peak anthropogenic heat emissions would be. Our results also align with similar findings for low-rise residential areas elsewhere. For example, air conditioner use in the different climate of Osaka, Japan is predicted to increase both anthropogenic heat emissions of 25 W m^{-2} and outdoor air temperature of 0.1 °C (Kikegawa et al., 2022), despite the different types of climate. Such difference is relatively small but non-negligible, relative to global surface warming (IPCC, 2022). It is crucial to understand all contributors to urban heat, especially as global cities aim to enhance their resilience against climate change and be aware of potentially complex dynamic feedbacks. Therefore, these findings have implications for policymaking in cities globally, particularly where strategies aim at deploying new decarbonisation technologies, mitigating heat island effects, and improving urban living conditions.

Compared to the well-studied air-conditioning cooling in summer, the impact of ASHPs for heating on urban microclimate is less understood. We find that replacing gas boilers with ASHPs can decrease the 2 m outdoor air temperature by up to 0.16 °C in the UK due to reduction in anthropogenic heat emissions by up to 11.1 W m^{-2}. This magnitude is similar to the temperature and anthropogenic heat increases observed in summer, although slightly larger air temperature changes occur in winter due to more stable conditions. These findings address a gap in the current understanding of ASHPs' effects on urban microclimate.

The change in air temperature to anthropogenic heat emission ratio ($\Delta T_2/\Delta Q_{F,B}$) is critical, as it captures the local-scale climate response or sensitivity to anthropogenic heat input, and allows inter-study comparisons (Wang et al., 2023). Despite different models, our $\Delta T_2/\Delta Q_{F,B}$ ratios (range: 0.004 to 0.014 °C (W m^{-2})$^{-1}$) in summer agree with previous research (Table 1), such as Bohnenstengel et al.'s (2014) London value (~0.008 °C (W m^{-2})$^{-1}$), Wang et al. (2018) for Hong Kong (~0.007 °C (W m^{-2})$^{-1}$) and Salamanca et al. (2014) for Phoenix (~0.008 °C (W m^{-2})$^{-1}$). Here, we observe the diurnal pattern of $\Delta T_2/\Delta Q_{F,B}$ typically has a U-shape, with lower daytime and higher nocturnal values. This pattern is primarily influenced by friction velocity and atmospheric stability. With more unstable conditions during the daytime, the friction velocity is greater, resulting in a smaller $\Delta T_2/\Delta Q_{F,B}$. Whilst at night, the atmospheric stability may be neutral or stable reducing the friction velocity, consequently increasing $\Delta T_2/\Delta Q_{F,B}$. Similarly, stable conditions are more common in winter than in summer, leading to larger overall $\Delta T_2/\Delta Q_{F,B}$ in winter. This atmospheric stability canopy aerodynamic resistance feedback has been noted by others (e.g. Wang et al. (2023)).

We focus on low-rise residential neighbourhoods, with their distinct thermal characteristics and energy consumption patterns are central to recent government sustainable urban development policies. However, these areas are expected to exhibit different thermal behaviours compared to high-rise commercial districts. Despite their relatively smaller surface area, high-rise districts can generate significantly higher magnitudes of heat emission and local warming effects. This is exemplified in Hong Kong, where the $Q_{F,B}$ can reach up to 300 W m^{-2} with an area of 500 m $\times$ 500 m, and the T_2 may increase by up to 2 °C, maintaining a similar $\Delta T_2/\Delta Q_{F,B}$ ratio as observed in our studies (Wang et al., 2018). Furthermore, high-rise neighbourhoods are expected to have a larger boundary layer depth, increasing the volume heat and pollutants are mixed into and therefore potentially mitigating some local warming effects yet impacting broader atmospheric conditions. In cities, such spatial variability patterns—where a small, densely built commercial area generates much larger anthropogenic heat than the majority residential area—can exacerbate inequalities. Temperature increases caused by regions producing large amounts of anthropogenic heat may

affect nearby regions producing less (Xu et al., 2024). This could be further studied in future works.

There are uncertainties associated with the data and models used in this study. We consider idealised neighbourhoods with identical residential building archetypes. Although the archetypes are based on the most common building types in recent housing surveys, they may not represent future reality. Our future scenario assumes post-1996 buildings, with better insulation, higher air tightness, and hence smaller cooling and heating demand, resulting in less anthropogenic heat emissions than older buildings (Liu et al., 2023; Xu et al., 2024). Therefore, neighbourhoods with fewer retrofitted old buildings, the anthropogenic heat emission and resulting outdoor air temperature changes could be underpredicted.

Additionally, our assumptions neglect other types of anthropogenic heat. While outdoor metabolism may be minimal, anthropogenic heat from road traffic can be relatively large especially during peak hours on weekdays if busy roads are in the vicinity. =Iamarino et al. (2012) found that in London from 2005 to 2008, the anthropogenic heat generated by road transportation was about one-third of that generated by residential buildings. Therefore, it may contribute to the increase in outdoor air temperature, subsequently increasing/decreasing the building cooling/heating load and the feedback effect on outdoor air temperature, although the magnitude can be still small in the UK context. However, this is the not the focus of the current study.

This study demonstrates a method that could be expanded to broader applications in the future. As SUEWS only requires commonly available input data, this method is adaptable to other locations globally. It is particularly relevant for countries expecting an increase in building cooling demand. For example, northern European countries with high adoption rates of air source heat pumps and rising indoor overheating risks due to climate change (Taylor et al., 2023), as well as countries with hot climates with low air conditioners usage but increasing adoption rates, like Sri Lanka (Blunn et al., 2024).

Due to the low computational demands, the SUEWS-EnergyPlus approach can be applied to cover large areas with higher spatial resolution (order 100 m) compared to existing studies (Table 1). This will provide a better understanding of the temporal and spatial variability of building energy use, anthropogenic heat emissions, and the resultant warming effects across the city.

5. Conclusions

The UK is rolling out ASHPs for residential buildings to drive decarbonisation and achieve net zero by 2050. With global warming, ASHPs are expected to be increasingly relied upon for both cooling and heating in the UK. The impact of anthropogenic heat emissions from ASHPs on urban thermal environments can be significant, but their effects in future UK scenarios remain underexplored. Additionally, previous studies often use meso-scale climate models with BEP/BEM, which has limitations in capturing detailed building characteristics such as geometry, space types and occupancy behaviours.

To address these gaps, this study introduces a novel approach by combining the local-scale land surface model SUEWS with the detailed building energy simulation tool EnergyPlus with two-way coupling. This SUEWS-EnergyPlus modelling scheme comprehensively assesses ASHPs' impact on urban temperatures in various UK residential neighbourhoods under the 2050s future climate. By including detailed building-scale simulations alongside analyses of two-way feedback between the urban climate and buildings, this approach balances computational cost and accuracy, allowing for quick and specific assessments of neighbourhood buildings.

Our results show that the influence of ASHP on outdoor temperatures in the UK low-rise residential neighbourhoods is relatively minor. In summer, the maximum increase in building anthropogenic heat emission $\Delta Q_{F,B}$ is up to 6.4 W m^{-2} for detached houses and 19.3 W m^{-2} for flats. The corresponding outdoor 2 m air temperature T_2 rises are up to around 0.03 °C and 0.12 °C, respectively. In winter, replacing gas boilers with ASHPs reduces $Q_{F,B}$ by up to 5.6 W m^{-2} for detached houses and 11.1 W m^{-2} for flats, leading to decreases in decrease in T_2 of up to 0.08 °C and 0.16 °C. Typically the $\Delta T_2/\Delta Q_{F,B}$ diurnal pattern has smaller values during the daytime and higher values at night. Seasonally, $\Delta T_2/\Delta Q_{F,B}$ is higher in winter than in summer. These patterns are mainly influenced by friction velocity and therefore the atmospheric stability.

We find that the variability in $\Delta Q_{F,B}$ from replacing gas boilers with ASHPs and resultant ΔT_2 aligns with regional differences in outdoor air temperature in the UK. London, with its warmer climate, has the highest increases in $Q_{F,B}$ and T_2 in summer, while for cooler Aberdeen, the decreases in $Q_{F,B}$ and T_2 are the largest in winter. The local climate sensitivity to anthropogenic heat change, represented by the ratio $\Delta T_2/\Delta Q_{F,B}$, is largely consistent across various UK climates.

While this study focuses on the UK, it addresses a common challenge faced by countries and cities globally: balancing the adoption of emerging technologies with their potential negative impacts on the urban environment. Understanding all contributors to urban heat is crucial as cities aim to enhance their resilience against climate change and foresee the various complex effects associated with it.

Future work could involve applying the SUEWS-EnergyPlus modelling scheme to broader scenarios, for example creating high-resolution maps of building anthropogenic heat emissions that covers various neighbourhood types like high-rise commercial areas. Our modelling method and findings should be valuable for policymakers and urban planners in the UK and globally. These insights are crucial for planning building electrification and decarbonisation, which are essential pathways to achieving net zero emissions.

CRediT authorship contribution statement

Xiaoxiong Xie: Writing – review & editing, Writing – original draft, Visualization, Software, Methodology, Investigation. **Zhiwen Luo:** Writing – review & editing, Supervision, Methodology, Funding acquisition, Conceptualization. **Sue Grimmond:** Writing – review & editing, Methodology, Funding acquisition. **Yiqing Liu:** Writing – review & editing, Methodology. **Carlos E. Ugalde-Loo:** Writing – review & editing, Funding acquisition. **Matthew T. Bailey:** Writing – review & editing, Funding acquisition. **Xinfang Wang:** Writing – review & editing, Funding acquisition.

Declaration of competing interest

The authors declare that they have no known competing financial interests or personal relationships that could have appeared to influence the work reported in this paper.

Data availability

Information on the data underpinning the results presented here can be found at https://doi.org/10.5281/zenodo.13351764.

Acknowledgements

This work has been funded by EPSRC-H + C Zero Network (EP/T022906/1; HC2-005), NERC-COSMA (NE/S005889/1), NERC-ASSURE (NE/W002965/1) and ERC urbisphere (85505).

Supplementary materials

Supplementary material associated with this article can be found, in the online version, at doi:10.1016/j.scs.2024.105811.

References

Abela, A., Hamilton, L., Hitchin, R., Lewry, A., Pout, C., 2016. BRE Client Report for the Department of Energy & Climate Change - Study on Energy Use by Air-Conditioning: Final Report. London, UK.

Ao, X., Grimmond, C. S. B., Ward, H. C., Gabey, A. M., Tan, J., Yang, X. Q., & Zhang, N. (2018). Evaluation of the Surface Urban Energy and Water Balance Scheme (SUEWS) at a Dense Urban Site in Shanghai: Sensitivity to Anthropogenic Heat and Irrigation. *Journal of Hydrometeorololy, 19*, 1983–2005.

Arnfield, A. J., & Grimmond, C. S. B. (1998). An urban canyon energy budget model and its application to urban storage heat flux modeling. *Energy and Buildings, 27*, 61–68.

Bastin, J. F., Clark, E., Elliott, T., Hart, S., van den Hoogen, J., Hordijki, I., & Crowther, T. W. (2019). Understanding climate change from a global analysis of city analogues. *PLoS. One, 14*, Article e0217592.

Battini, F., Pernigotto, G., & Gasparella, A. (2023). A shoeboxing algorithm for urban building energy modeling: Validation for stand-alone buildings. *Sustainable Cities Society., 89*, Article 104305.

BEIS, 2021. Net Zero Strategy: Build Back Greener, Gov.Uk.

BIES, 2021. Cooling in the UK.

Blunn, L., Xie, X., Grimmond, S., Luo, Z., Sun, T., Perera, N., & Emmanuel, R. (2024). Spatial and temporal variation of anthropogenic heat emissions in Colombo, Sri Lanka. *Urban. Clim., 54*, Article 101828.

Bohnenstengel, S. I., Hamilton, I., Davies, M., & Belcher, S. E. (2014). Impact of anthropogenic heat emissions on London's temperatures. *Quarterly Journal of the Royal Meteorological Society, 140*, 687–698.

Brousse, O., Simpson, C., Zonato, A., Martilli, A., Taylor, J., Davies, M., & Heaviside, C. (2024). Cool Roofs Could Be Most Effective at Reducing Outdoor Urban Temperatures in London (United Kingdom) Compared With Other Roof Top and Vegetation Interventions: A Mesoscale Urban Climate Modeling Study. *Geophysical research letters, 51*, Article e2024GL109634.

Chen, W., Zhou, Y., Xie, Y., Chen, G., Ding, K. J., & Li, D. (2022). Estimating spatial and temporal patterns of urban building anthropogenic heat using a bottom-up city building heat emission model. *Resour. Conserv. Recycl., 177*, Article 105996.

Chow, D. H., Beng, B., Mashrae, M., Levermore, G. J., Arcs, B., Dic, P., & Mashrae, F. (2010). The effects of future climate change on heating and cooling demands in office buildings in the UK. *Building Services Engineering Research and Technology, 31*, 307–323.

Chua, K. J., Chou, S. K., & Yang, W. M. (2010). Advances in heat pump systems: A review. *Applied Energy, 87*, 3611–3624.

CIBSE, 2014. CIBSE TM49: Design Summer Years for London. London, UK.

CIBSE, 2021. AM16 Heat pump installations for multi-unit residential buildings.

Climate Change Committee. (2020). The Sixth Carbon Budget: The UK's path to Net Zero. *The Carbon Budget*.

Cuerda, E., Guerra-Santin, O., Sendra, J. J., & Neila González, Fco. J. (2019). Comparing the impact of presence patterns on energy demand in residential buildings using measured data and simulation models. *Build. Simul., 12*, 985–998.

De Munck, C., Pigeon, G., Masson, V., Meunier, F., Bousquet, P., Tréméac, B., & Marchadier, C. (2013). How much can air conditioning increase air temperatures for a city like Paris, France? *International Journal of Climatology, 33*, 210–227.

Department for Communities and Local Government, 2013English housing survey: Headline report 2011–12.

Department for Energy Security and Net Zero, 2023. Changes to the Boiler Upgrade Scheme, October 2023 [WWW Document]. URL https://www.gov.uk/government/publications/boiler-upgrade-scheme-changes-to-grant-levels/changes-to-the-boiler-upgrade-scheme-october-2023 (accessed 4.26.24).

DERFA, 2009. Adapting to climate change: UK climate projections 2009, Uk Climate Projections. London, UK.

Eames, M., Kershaw, T., & Coley, D. (2011). On the creation of future probabilistic design weather years from UKCP09. *Building Services Engineering Research and Technology, 32*, 127–142.

Ferrando, M., Hong, T., & Causone, F. (2021). A simulation-based assessment of technologies to reduce heat emissions from buildings. *Build. Environ., 195*, Article 107772.

Grimmond, C. S. B., & Oke, T. R. (1999). Heat Storage in Urban Areas: Local-Scale Observations and Evaluation of a Simple Model. *Journal of Applied Meteorology, 38*, 922–940.

Grimmond, S. (1992). The suburban energy balance: Methodological considerations and results for a mid-latitude west coast city under winter and spring conditions. *International Journal of Climatology, 12*, 481–497.

Gutiérrez, E., González, J. E., Martilli, A., & Bornstein, R. (2015). On the Anthropogenic Heat Fluxes Using an Air Conditioning Evaporative Cooling Parameterization for Mesoscale Urban Canopy Models. *Journal of Solar Energy Engineering, 137*.

Harman, I. N., & Finnigan, J. J. (2008). Scalar Concentration Profiles in the Canopy and Roughness Sublayer. *Boundary-Layer Meteorology, 129*, 323–351.

Hersbach, H., Bell, B., Berrisford, P., Hirahara, S., Horányi, A., Muñoz-Sabater, J., & Thépaut, J. N. (2020). The ERA5 global reanalysis. *Quarterly Journal of the Royal Meteorological Society, 146*, 1999–2049.

Hong, T., Ferrando, M., Luo, X., & Causone, F. (2020). Modeling and analysis of heat emissions from buildings to ambient air. *Applied Energy, 277*, Article 115566.

Iamarino, M., Beevers, S., & Grimmond, C. S. B. (2012). High-resolution (space, time) anthropogenic heat emissions: London 1970–2025. *International Journal of Climatology, 32*, 1754–1767.

IEA, 2021. Net Zero by 2050: A Roadmap for the Global Energy Sector.

IEA, 2022a. Global Energy Review: CO2 Emissions in 2021.

IEA, 2022b. The Future of Heat Pumps.

IEA, 2024. Heat Pumps [WWW Document]. URL https://www.iea.org/energy-system/buildings/heat-pumps (accessed 8.7.24).

IPCC. (2022). Buildings. *Climate change 2022 - Mitigation of climate change* (pp. 953–1048). Cambridge, UK and New York, NY, USA: Cambridge University Press.

Järvi, L., Grimmond, C. S. B., & Christen, A. (2011). The Surface Urban Energy and Water Balance Scheme (SUEWS): Evaluation in Los Angeles and Vancouver. *J. Hydrol. (Amst), 411*, 219–237.

Kikegawa, Y., Genchi, Y., Yoshikado, H., & Kondo, H. (2003). Development of a numerical simulation system toward comprehensive assessments of urban warming countermeasures including their impacts upon the urban buildings' energy-demands. *Applied Energy, 76*, 449–466.

Kikegawa, Y., Nakajima, K., Takane, Y., Ohashi, Y., & Ihara, T. (2022). A quantification of classic but unquantified positive feedback effects in the urban-building-energy-climate system. *Applied energy, 307*, Article 118227.

Kokkonen, T. V., Grimmond, C. S. B., Räty, O., Ward, H. C., Christen, A., Oke, T. R., & Järvi, L. (2018). Sensitivity of Surface Urban Energy and Water Balance Scheme (SUEWS) to downscaling of reanalysis forcing data. *Urban. Clim., 23*, 36–52.

Kotthaus, S., & Grimmond, C. S. B. (2014). Energy exchange in a dense urban environment – Part I: Temporal variability of long-term observations in central London. *Urban. Clim., 10*, 261–280.

Lee, S. H., Hong, T., Le, M., Medina, L., Xu, Y., Robinson, A., & Piette, M. A. (2024). Assessment of energy and thermal resilience performance to inform climate mitigation of multifamily buildings in disadvantaged communities. *Sustain. Cities. Soc., 104*, Article 105319.

Lindberg, F., Grimmond, C. S. B., Gabey, A., Huang, B., Kent, C. W., Sun, T., & Zhang, Z. (2018). Urban Multi-scale Environmental Predictor (UMEP): An integrated tool for city-based climate services. *Environmental Modelling & Software, 99*, 70–87.

Liu, C. (2017). *Creation of hot summer years and evaluation of overheating risk at a high spatial resolution under a changing climate*. University of Bath.

Liu, Y., Luo, Z., & Grimmond, S. (2022). Revising the definition of anthropogenic heat flux from buildings: Role of human activities and building storage heat flux. *Atmospheric Chemistry and Physics (Print), 22*, 4721–4735.

Liu, Y., Luo, Z., & Grimmond, S. (2023). Impact of building envelope design parameters on diurnal building anthropogenic heat emission. *Build. Environ., 234*, Article 110134.

Meyn, S. K., & Oke, T. R. (2009). Heat fluxes through roofs and their relevance to estimates of urban heat storage. *Energy and Buildings, 41*, 745–752.

MHCLG, 2021. English Housing Survey 2019-2020.

Morales Sandoval, D. A., Saikia, P., De la Cruz-Loredo, I., Zhou, Y., Ugalde-Loo, C. E., Bastida, H., & Abeysekera, M. (2023). A framework for the assessment of optimal and cost-effective energy decarbonisation pathways of a UK-based healthcare facility. *Applied Energy, 352*, Article 121877.

Office for National Statistics. (2023). *Towns and cities, characteristics of built-up areas* (p. 2021). England and Wales: Census.

Ohashi, Y., Suido, M., Kikegawa, Y., Ihara, T., Shigeta, Y., & Nabeshima, M. (2016). Impact of seasonal variations in weekday electricity use on urban air temperature observed in Osaka. *Japan. Quarterly Journal of the Royal Meteorological Society, 142*, 971–982.

Omidvar, H., Sun, T., Grimmond, S., Bilesbach, D., Black, A., Chen, J., & McFadden, J. P. (2022). Surface Urban Energy and Water Balance Scheme (v2020a) in vegetated areas: Parameter derivation and performance evaluation using FLUXNET2015 dataset. *Geosci. Model. Dev., 15*, 3041–3078.

Pokhrel, R., Ramírez-Beltran, N. D., & González, J. E. (2019). On the assessment of alternatives for building cooling load reductions for a tropical coastal city. *Energy and Buildings, 182*, 131–143.

Porritt, S.M., 2012. Adapting uk dwellings for heat waves. De Montfort University.

Rigden, A., Li, D., & Salvucci, G. (2018). Dependence of thermal roughness length on friction velocity across land cover types: A synthesis analysis using AmeriFlux data. *Agricultural and Forest Meteorology, 249*, 512–519.

Roberts, D., Vera-Toscano, E., & Phimister, E. (2015). Fuel poverty in the UK: Is there a difference between rural and urban areas? *Energy Policy, 87*, 216–223.

Sailor, D. J. (2011). A review of methods for estimating anthropogenic heat and moisture emissions in the urban environment. *International Journal of Climatology, 31*, 189–199.

Sailor, D. J., & Vasireddy, C. (2006). Correcting aggregate energy consumption data to account for variability in local weather. *Environmental Modelling & Software, 21*, 733–738.

Salamanca, F., Georgescu, M., Mahalov, A., Moustaoui, M., & Wang, M. (2014). Anthropogenic heating of the urban environment due to air conditioning. *Journal of Geophysical Research: Atmospheres, 119*, 5949–5965.

Salamanca, F., Krpo, A., Martilli, A., & Clappier, A. (2010). A new building energy model coupled with an urban canopy parameterization for urban climate simulations-part I. formulation, verification, and sensitivity analysis of the model. *Theoretical and Applied Climatology, 99*, 331–344.

Soebarto, V., & Bennetts, H. (2014). Thermal comfort and occupant responses during summer in a low to middle income housing development in South Australia. *Build. Environ., 75*, 19–29.

Sun, T., & Grimmond, S. (2019). A Python-enhanced urban land surface model SuPy (SUEWS in Python, v2019.2): Development, deployment and demonstration. *Geosci. Model. Dev., 12*, 2781–2795.

Sun, T., Omidvar, H., Li, Z., Zhang, N., Huang, W., Kotthaus, S., & Grimmond, S. (2024). WRF (v4.0)-SUEWS (v2018c) coupled system: Development, evaluation and application. *Geoscience of Model. Development, 17*, 91–116.

Takane, Y., Kikegawa, Y., Hara, M., & Grimmond, C. S. B. (2019). Urban warming and future air-conditioning use in an Asian megacity: Importance of positive feedback. *npj Climate and Atmospheric Science, 2*, 1–11, 20191 2.

Tang, Y., Sun, T., Luo, Z., Omidvar, H., Theeuwes, N., Xie, X., & Grimmond, S. (2021). Urban meteorological forcing data for building energy simulations. *Building Environment, 204*, Article 108088.

Taylor, J., McLeod, R., Petrou, G., Hopfe, C., Mavrogianni, A., Castaño-Rosa, R., & Lomas, K. (2023). Ten questions concerning residential overheating in Central and Northern Europe. *Building Environment, 234*, Article 110154.

Theeuwes, N. E., Ronda, R. J., Harman, I. N., Christen, A., & Grimmond, C. S. B. (2019). Parametrizing horizontally-averaged wind and temperature profiles in the urban roughness sublayer. *Boundary-layer Meteorology, 173*, 321–348.

U.S. Department of Energy, 2020a. EnergyPlus | EnergyPlus [WWW Document]. URL https://energyplus.net/ (accessed 2.8.21).

U.S. Department of Energy, 2020b. EnergyPlus version 9.4.0 documentation: Input output reference.

UKERC, 2016. UKERC Technology and Policy Assessment.

UKERC, 2020. The pathway to net zero heating in the UK. London.

Wang, L., Gwilliam, J., & Jones, P. (2009). Case study of zero energy house design in UK. *Energy and Buildings, 41*, 1215–1222.

Wang, L., Sun, T., Zhou, W., Liu, M., & Li, D. (2023). Deciphering the sensitivity of urban canopy air temperature to anthropogenic heat flux with a forcing-feedback framework. *Environmental Research Letters, 18*, Article 094005.

Wang, Y., Li, Y., Di Sabatino, S., Martilli, A., & Chan, P. W. (2018). Effects of anthropogenic heat due to air-conditioning systems on an extreme high temperature event in Hong Kong. *Environmental Research Letters, 13*, Article 034015.

Ward, H. C., & Grimmond, C. S. B. (2017). Assessing the impact of changes in surface cover, human behaviour and climate on energy partitioning across Greater London. *Landscape and Urban Planning, 165*, 142–161.

Ward, H. C., Kotthaus, S., Järvi, L., & Grimmond, C. S. B. (2016). Surface Urban Energy and Water Balance Scheme (SUEWS): Development and evaluation at two UK sites. *Urban. Clim., 18*, 1–32.

WMO, 2000. IPCC Special report - emissions scenarios.

World Resources Institute. (2022). *Climate watch historical ghg emissions*. Washington, DC.

Xie, X., Luo, Z., Grimmond, S., & Blunn, L. (2023a). Use of wind pressure coefficients to simulate natural ventilation and building energy for isolated and surrounded buildings. *Building Environment, 230*, Article 109951.

Xie, X., Luo, Z., Grimmond, S., & Sun, T. (2023b). Impact of building density on natural ventilation potential and cooling energy saving across Chinese climate zones. *Building Environment, 244*, Article 110621.

Xie, X., Luo, Z., Grimmond, S., Sun, T., & Morrison, W. (2022). Impact of inter-building longwave radiative exchanges on building energy performance and indoor overheating. *Building Environment, 209*, Article 108628.

Xu, X., González, J. E., Shen, S., Miao, S., & Dou, J. (2018). Impacts of urbanization and air pollution on building energy demands — Beijing case study. *Applied Energy, 225*, 98–109.

Xu, Y., Vahmani, P., Jones, A., & Hong, T. (2024). Anthropogenic heat from buildings in Los Angeles County: A simulation framework and assessment. *Sustainable Cities. Society, 107*, Article 105468.

Yan, D., O'Brien, W., Hong, T., Feng, X., Burak Gunay, H., Tahmasebi, F., & Mahdavi, A. (2015). Occupant behavior modeling for building performance simulation: Current state and future challenges. *Energy and Buildings, 107*, 264–278.